INSTABILITY OF CYLINDRICAL SHELLS WITH INCLINED STIFFENERS

By
RU - LIN LEE

A DISSERTATION PRESENTED TO THE GRADUATE COUNCIL OF
THE UNIVERSITY OF FLORIDA
IN PARTIAL FULFILLMENT OF THE REQUIREMENTS FOR THE
DEGREE OF DOCTOR OF PHILOSOPHY

UNIVERSITY OF FLORIDA
August, 1965

ACKNOWLEDGMENTS

The author wishes to express his sincere gratitude to all the members of his supervisory committee. In particular, he wishes to thank Dr. S. Y. Lu, Chairman of his supervisory committee, for constant advice and encouragement throughout the entire period of this research. He would also like to thank Dr. William A. Nash, Chairman, Department of Engineering Science and Mechanics, for his valuable suggestions and financial support throughout the author's entire graduate-study program.

He is also indebted to Dr. I. K. Ebcioglu, Department of Engineering Science and Mechanics, Dr. J. Siekmann, Department of Engineering Science and Mechanics, and Dr. R. G. Blake, Department of Mathematics, for serving on his supervisory committee and for the various stimulating discussions he has held with them over the past few years.

Final thanks go to the National Aeronautics and Space Administration for their sponsorship of this study.

TABLE OF CONTENTS

TABLE OF CONTENTS (Continued)

LIST OF TABLES

LIST OF FIGURES

LIST OF FIGURES (Continued)

LIST OF SYMBOLS

D	Flexural rigidity of the shell $= \frac{Et^3}{12(1-\nu^2)}$
E	Young's modulus for shell
E_j, E_k	Young's modulus for j^{th} and k^{th} stiffeners, respectively
$\bar{E}_j$, $\bar{E}_k$	Dimensionless Young's modulus for j^{th} and k^{th} stiffeners, respectively
G_j, G_k	Shear modulus for j^{th} and k^{th} stiffeners
$\bar{G}_j$, $\bar{G}_k$	Dimensionless shear modulus for j^{th} and k^{th} stiffeners, respectively
I_j, I_k	Moment of inertia of j^{th} and k^{th} stiffeners about center of gravity of j^{th} and k^{th} stiffeners respectively
$\bar{I}_j$, $\bar{I}_k$	Dimensionless moment of inertia of j^{th} and k^{th} stiffeners about center of gravity of j^{th} and k^{th} stiffeners respectively
J_j, J_k	Polar moment of inertial of j^{th} and k^{th} stiffeners
$\bar{J}_j$, $\bar{J}_k$	Dimensionless polar moment of inertial of j^{th} and k^{th} stiffeners
K	Torsional rigidity of the stiffeners
L	Length of the shell
ℓ	Total length of stiffeners
m, n	Numbers of waves in the axial and circumferential directions
N_k	Number of stiffeners in γ_1-direction

N_j	Number of stiffeners in γ_2-direction
P	Transverse load
p	Internal pressure
Pc	Axial load
$\overline{P}$	Dimensionless transverse load
$\overline{p}$	Dimensionless internal pressure
R	Radius of the shell
t	Thickness of shell
t_1	Thickness of stiffeners
u, v, w	Components of displacements in x, y, z directions, respectively. Fig. 1
w_o	Initial deflection
x, y, z	Orthogonal coordinates on median surface of shell
β	Dimensionless parameter defined in Eq. (22)
Γ	Imperfection ratio = $\frac{w_o}{w}$
γ_1, γ_2	The angles between the stiffeners and the generator of the cylinder, respectively
η, η_1	Ratio of arbitrary parameters defined in Eq. (48)
μ	Ratio of numbers of waves in the circumferential and axial direction
ν	Poisson's ratio for shell

σ_c, σ_b, σ	Average axial compression stress, bending stress, and eccentric compression stress, respectively
$\bar{\sigma}_c$, $\bar{\sigma}_b$, $\bar{\sigma}$	Dimensionless axial compression stress, bending stress, and eccentric compression stress, respectively
∇^2	Laplace operator
∇^4	Biharmonic operator = $(\nabla^2)^2$

Abstract of Dissertation Presented to the Graduate Council in Partial Fulfillment of the Requirements for the Degree of Doctor of Philosophy

INSTABILITY OF CYLINDRICAL SHELLS WITH INCLINED STIFFENERS

By

Ru-Lin Lee

August, 1965

Chairman: Dr. S. Y. Lu

Major Department: Engineering Science and Mechanics

An analytic study of the general stability of thin circular cylindrical shells stiffened by a system of inclined stiffeners has been carried out. The cylinder is internally pressurized and is under three types of loadings, namely, axial compression, bending, and transverse shear load. The stiffeners are not very close but are discretely located and the eccentricity of stiffeners is disregarded. The method of the solution is carried out by the use of nonlinear large deflection theory and the effects of initial imperfections in the strain-displacement equations are considered. The Ritz-method is used

to find the governing equations of instability of stiffened shells subject to the three types of loading.

Numerical examples for cylinders with inclined stiffeners at different angles are worked out. The minimum strength of shell versus different rigidities of stiffener are also calculated. The relation between the minimum strength of pressurized shell and internal pressure is plotted. The computation was carried out on the IBM 709. Some tests have been made on the shell with inclined stiffeners at angles of $\gamma = 30^{\circ}$, 45°, and 60° under axial compression and bending loads. Some of the experimental data are plotted to compare with the analytical results.

CHAPTER I

INTRODUCTION

Interest in shell buckling phenomena dates back to 1858 when Fairbairn (1)* performed his experiments on the buckling of cylinders under uniform external pressure. In 1888, the first theoretical treatment of the problem was published by Bryan (2) and Love (3), and since that time, many investigators have been attracted to the various problems of thin shell instability. The equations for thin shells were discussed by Timoshenko (4) in his well-known book. The study of stability of isotropic cylindrical shells was advanced by Southwell (5). In 1933, a set of equilibrium equations for cylindrical shells subject to torsion was derived by Donnell (6) based on the theory of small deflections. A simplified method of elastic-stability analysis for thin cylindrical shells was also discussed by Batdrof (7).

---

*Underlined numbers in parentheses refer to entries in the references.

Then Suer and Harris (8) applied Donnell's eighth-order linear equilibrium equation to the problem of the stability of cylinders under combined torsion and hydrostatic pressure. They obtained a solution with Galerkin's method based on an assumed radial deflection function in the form of an infinite trigonometric series.

In 1961, Seide (9) had presented an analysis of the buckling of cylindrical shells subject to pure bending. However, these classical analyses are valid only for infinitesimal deflection. When the deflection is not very small and has a magnitude of wall-thickness, large deflection theory must be used, and the high order terms of deflection are to be considered. In general, small deflection theory predicts buckling stresses approximately three times as great as those found by experiments. This evidence is particularly obvious for cylindrical shells under axial compression. The discrepancy between the small deflection and experimental results can be explained by use of large deformation theory which was advanced by Donnell (10) and von Karman and Tsien (11). In Ref. (10), Donnell also considered the initial imperfection in the shell to cause lower buckling load. A diamond-shaped buckling pattern represented by a function

of arbitrary parameters was first proposed by von Karman and Tsien (11) for cylindrical shell under axial compression. Their results agreed with the experimental results. The same problem was also solved by Kempner (12) who used the Ritz-method, but improved the von Karman and Tsien's solution by considering five free parameters. An investigation of the buckling of cylindrical shells by use of Galerkin's method was also studied by Ekstrom (13) and Lu and Nash (14). The general case of the axially compressed orthotropic and isotropic cylinder with internal pressure has been discussed by Thielemann (15). The general equations in tensor notation for isotropic shells were derived by Dill (16) who also included the effect of initial imperfections. The effect of initial imperfection on the buckling of cylinders under different loadings was studied in Ref. (17), (18), (19), (20), (21) and (22).

The general instability of ring-stiffened or stringer-stiffened cylindrical shell by the use of small-deflection relations have been investigated by many authors, Nash (23), Alfutov (24), McKenzie (25) and Kan and Lipovskiy (26). Further study in general instability of ring-stiffened cylindrical shells subject to external hydrostatic pressure with a comparison of theory and experiment was discussed by Galletly, Slankard and Wenk (27).

A detailed treatment of the buckling of stiffened shells has been discussed by Hedgepeth and Hall (28). The problem of stability of orthotropic shells was studied by Becker and Gerard (29). Further study in general instability of orthogonally stiffened plates or cylindrical shells has been discussed by Huffington, Jr. (30), Neut (31) and Becker (32).

In Ref. (32), an analysis of orthotropic cylinders was made by Taylor whose derivations were based upon the use of a form of Donnell's equation. Recently, an analytical investigation on the instability modes of orthotropic cylinders subject to compressive or bending load was made by Block (33). He used the Dirac delta function for rings in the linear equilibrium equation and considered the pressure load.

The large deflection relations applied to the problem of the instability of ring-stiffened cylindrical shells derived energy method was investigated by Lee (34).

Experimental work on the ring-stiffened cylinders or unstiffened cylinders under different loadings has been performed by MaCoy (35), Peterson and Dow (36), Lundquist (37), Harris (38), Fung (39), and Goree (40).

The theory of anisotropic elasticity has been discussed by Hearmon (41) and Lekhnitsky (42). A general discussion on the theory of anisotropic shells has been made by Ambartsumyan (43). A linear solution of anisotropic cylinders was investigated by Cheng and Ho (44).

The purpose of this study is to investigate the general instability of cylindrical shells with a system of stiffeners which is mounted at various angles. The cylinder is internally pressurized and under one of the following types of loading:

a. Uniform axial compression

b. Uniform bending

c. Uniform transverse load.

The stiffeners are not very close but discretely located and thus the anisotropic relation does not apply. The Kirchnoff hypothesis is assumed; the eccentricity of stiffeners disregarded. The method of the solution is first to assume the deflection function, then the stress function is found from compatibility equation which is carried out by the use of nonlinear large deflection theory. The expressions for the energy stored in the shell and stiffeners as well as the work due to the external loads are obtained. The large deflection terms and the effect of initial imperfections in the strain displacement

equations are considered. The Ritz-method is used to find the governing equations of instability of stiffened shells subject to these three types of loading used. Hence, the minimum loads are found from these equations.

Numerical examples are worked out for the cylinders with the inclined stiffeners at different angles. The minimum strength of shell versus different rigidities of stiffener is also calculated. The relation between the minimum strength of pressurized shell and internal pressure is plotted in Fig. 15. The computation was carried out on the IBM 709. The general computer programs written in Fortran II to find these minimum stresses for all three types of loading are listed in Appendix B. Some tests have been made on the shell with inclined stiffeners at angles of $\gamma = 30^{\circ}$, 45°, and 60° under axial compression and bending load. Some of the experimental data are plotted in Fig. 18 to compare with the theoretical results.

CHAPTER II

BASIC RELATIONS

2.1 Compatibility Equations

In the present investigation, the following assumptions are made:

a. Elements normal to the unstrained middle surface of the shell remain normal to the strained middle surface.

b. The material follows Hooke's Law.

Let x and y be measured in the axial and the circumferential direction in the median surface of the underformed cylindrical shell (Fig. 1), w equal the total radial deflection, and w_o represent the initial deflection in the radial direction. The strain-displacement relations are (22):

$$\epsilon_x = \frac{\partial u}{\partial x} + \frac{1}{2}\left(\frac{\partial w}{\partial x}\right)^2 - \frac{1}{2}\left(\frac{\partial w_o}{\partial x}\right)^2$$

$$\epsilon_y = \frac{\partial v}{\partial y} + \frac{1}{2}\left(\frac{\partial w}{\partial y}\right)^2 - \frac{1}{2}\left(\frac{\partial w_o}{\partial y}\right)^2 - \left(\frac{w - w_o}{R}\right)$$

$$\epsilon_{xy} = \frac{\partial u}{\partial y} + \frac{\partial v}{\partial x} + \frac{\partial w}{\partial x}\cdot\frac{\partial w}{\partial y} - \frac{\partial w_o}{\partial x}\cdot\frac{\partial w_o}{\partial y} \qquad (1)$$

In the above relations, the higher order terms of derivatives involving u and v are neglected, since these displacements are small compared to the radial displacement w.

The stresses and the strains in the median surface of the shell in the case of plane stress are related to each other by the following equations:

$$\sigma_x = \frac{E}{1-\nu^2}\,(\epsilon_x + \nu\,\epsilon_y)$$

$$\sigma_y = \frac{E}{1-\nu^2}\,(\epsilon_y + \nu\,\epsilon_x)$$

$$\sigma_{xy} = \frac{E}{2(1+\nu)}\,\epsilon_{xy} \qquad (2)$$

By substituting Eqs. (1) into Eqs. (2), the median surface stress-displacement relations are obtained:

$$\sigma_x = \frac{E}{1-\nu^2}\left\{\frac{\partial u}{\partial x} + \frac{1}{2}\left(\frac{\partial w}{\partial x}\right)^2 - \frac{1}{2}\left(\frac{\partial w_o}{\partial x}\right)^2 + \nu\left[\frac{\partial v}{\partial y} + \frac{1}{2}\left(\frac{\partial w}{\partial y}\right)^2 - \frac{1}{2}\left(\frac{\partial w_o}{\partial y}\right)^2 - \left(\frac{w-w_o}{R}\right)\right]\right\}$$

$$\sigma_y = \frac{E}{1-\nu^2}\left\{\frac{\partial v}{\partial y} + \frac{1}{2}\left(\frac{\partial w}{\partial y}\right)^2 - \frac{1}{2}\left(\frac{\partial w_o}{\partial y}\right)^2 - \left(\frac{w-w_o}{R}\right) + \nu\left[\frac{\partial u}{\partial x} + \frac{1}{2}\left(\frac{\partial w}{\partial x}\right)^2 - \frac{1}{2}\left(\frac{\partial w_o}{\partial x}\right)^2\right]\right\}$$

$$\sigma_{xy} = \frac{E}{2(1+\nu)}\left[\frac{\partial u}{\partial y} + \frac{\partial v}{\partial x} + \frac{\partial w}{\partial x}\frac{\partial w}{\partial y} - \frac{\partial w_o}{\partial x}\frac{\partial w_o}{\partial y}\right] \qquad (3)$$

The conditions of equilibrium can be satisfied by using the well-known Airy stress function F which is defined as

$$\sigma_x = \frac{\partial^2 F}{\partial y^2} \quad , \quad \sigma_y = \frac{\partial^2 F}{\partial x^2} \quad , \quad \sigma_{xy} = -\frac{\partial^2 F}{\partial x \partial y} \tag{4}$$

Eliminating the variables u and v in Eqs. (3) and (4), the following relation between stress function F and the radial component of the displacement w is obtained.

$$\left(\frac{\partial^2}{\partial x^2} + \frac{\partial^2}{\partial y^2}\right)^2 F = E\left[\left(\frac{\partial^2 w}{\partial x \partial y}\right)^2 - \frac{\partial^2 w}{\partial x^2} \cdot \frac{\partial^2 w}{\partial y^2} + \frac{\partial^2 w_o}{\partial x^2} \cdot \frac{\partial^2 w_o}{\partial y^2} - \frac{1}{R} \cdot \frac{\partial^2 w}{\partial x^2} + \frac{1}{R} \frac{\partial^2 w_o}{\partial x^2} - \left(\frac{\partial^2 w_o}{\partial x \partial y}\right)^2\right] \tag{5}$$

This equation expresses the condition of compatibility between stress and strain. It was first obtained in the present form by Donnell (10).

In general, w_o is unknown. For simplicity, w is assumed to be proportional to w_o Ref. (10), (17), (20), and (22) .. Thus one can define

$$\Gamma = \frac{w_o}{w} = \text{imperfection ratio} \tag{6}$$

where Γ is independent of x and y. With the relation from Eqs. (5), (6), the compatibility equation is expressed as:

$$\left(\frac{1}{1-\Gamma}\right)\nabla^4 F = E(1+\Gamma)\left[\left(\frac{\partial^2 w}{\partial x\,\partial y}\right)^2 - \frac{\partial^2 w}{\partial x^2}\cdot\frac{\partial^2 w}{\partial y^2}\right] - \frac{E}{R}\cdot\frac{\partial^2 w}{\partial x^2} \tag{7}$$

2.2 Energy Expressions

The strain energy in the shell and stiffeners and the potentials due to external load are found below.

a. The extensional strain energy in the shell can be written as:

$$U_e = \frac{t}{2E}\int_0^L\int_0^{2\pi R}\left\{\left(\frac{\partial^2 F}{\partial x^2}+\frac{\partial^2 F}{\partial y^2}\right)^2 + 2(1+\nu)\left[\left(\frac{\partial^2 F}{\partial x\,\partial y}\right)^2 - \frac{\partial^2 F}{\partial x^2}\cdot\frac{\partial^2 F}{\partial y^2}\right]\right\} dx\,dy \tag{8}$$

b. The bending strain energy has the following expression:

$$U_b = \frac{D}{2}\int_0^L\int_0^{2\pi R}\left[\left(\frac{\partial^2 w}{\partial x^2}-\frac{\partial^2 w_0}{\partial x^2}\right)^2 + 2\nu\left(\frac{\partial^2 w}{\partial x^2}-\frac{\partial^2 w_0}{\partial x^2}\right)\cdot\left(\frac{\partial^2 w}{\partial y^2}-\frac{\partial^2 w_0}{\partial y^2}\right) + \left(\frac{\partial^2 w}{\partial y^2}-\frac{\partial^2 w_0}{\partial y^2}\right)^2 + 2(1-\nu)\left(\frac{\partial^2 w}{\partial x\,\partial y}-\frac{\partial^2 w_0}{\partial x\,\partial y}\right)^2\right] dx\,dy \tag{9}$$

where

$$D = \frac{E\,t^3}{12(1-\nu^2)}$$

c. The potential due to edge bending of the shell is

$$U_m = -t\int_0^L\int_0^{2\pi R} \sigma_b\left[\cos\frac{y}{R}\cdot\frac{\partial u}{\partial x}\right]dx\,dy \tag{10}$$

where σ_b is applied peak bending stress and

$$\frac{\partial u}{\partial x} = \frac{1}{E}\left(\frac{\partial^2 F}{\partial y^2} - \nu\frac{\partial^2 F}{\partial x^2}\right) - \frac{1}{2}\left(\frac{\partial w}{\partial x}\right)^2 + \frac{1}{2}\left(\frac{\partial w_o}{\partial x}\right)^2$$

d. The work of the external force applied at the ends of the shell can be calculated as the product of the applied force and the change in length of the shell as follow:

$$U_c = \sigma_c t\int_0^L\int_0^{2\pi R}\left[\frac{1}{E}\left(\frac{\partial^2 F}{\partial y^2} - \nu\frac{\partial^2 F}{\partial x^2}\right) - \frac{1}{2}\left(\frac{\partial w}{\partial x}\right)^2 + \frac{1}{2}\left(\frac{\partial w_o}{\partial x}\right)^2\right]dx\,dy \tag{11}$$

where σ_c is constant stress over the shell thickness.

e. The potential due to the internal pressure p is

$$U_p = \int_0^L\int_0^{2\pi R} p\,(w - w_o)\;dx\,dy \tag{12}$$

The change in volume due to the displacements u, v are neglected (11).

f. The potential due to the edge bending on fixed end by transverse shear load P which applied at the free end (Fig. 3) is

$$U_P = -\int_0^L \int_0^{2\pi R} \left(\frac{P}{\pi R^2} x \cos \frac{y}{R} \cdot \frac{\partial u}{\partial x} \right) dx\,dy$$

$$= -\frac{P}{\pi R^2} \int_0^L \int_0^{2\pi R} x \cos \frac{y}{R} \left[\frac{1}{E} \left(\frac{\partial^2 F}{\partial y^2} - \nu \frac{\partial^2 F}{\partial x^2} \right) - \frac{1}{2} \left(\frac{\partial w}{\partial x} \right)^2 + \frac{1}{2} \left(\frac{\partial w_o}{\partial x} \right)^2 \right] dx\,dy \qquad (13)$$

g. The potential due to transverse shear load P applying on free end is

$$U_S = -\int_0^L \int_0^{2\pi R} \frac{P}{\pi R} \sin \frac{y}{R} \left(\frac{\partial u}{\partial y} + \frac{\partial v}{\partial x} \right) dx\,dy$$

$$= -\frac{P}{\pi R} \int_0^L \int_0^{2\pi R} \sin \frac{y}{R} \left[-\frac{2(1+\nu)}{E} \frac{\partial^2 F}{\partial x \partial y} - \frac{\partial w}{\partial x} \cdot \frac{\partial w}{\partial y} + \frac{\partial w_o}{\partial x} \cdot \frac{\partial w_o}{\partial y} \right] dx\,dy \qquad (14)$$

where P is average transverse shear load.

h. The bending strain energy of stiffeners. The stiffeners are assumed in parallel with the y_1, y_2 coordinates lines and the principal directions of the cylindrical shell coincide with x, y lines (Fig. 2). Let the subscript k be used for k^{th} stiffener which is inclined at an angle γ_1 with the generator of the cylinders, and is parallel with y_1 - line and normal to y'_2 - line. Thus the bending strain energy in the k^{th} stiffener is

$$U_{b,k} = \sum_{k=1}^{N_k} \frac{E_k I_k}{2} \int_0^{l_k} \left(\frac{\partial^2 w}{\partial y_1^2} - \frac{\partial^2 w_o}{\partial y_1^2} \right)^2_{y'_2=0} dy_1 \qquad (15)$$

where N_k denotes the number of the stiffeners in γ_1 - direction, and E_k I_k, represent Young's modulus and the moment of inertia of the k^{th} stiffener, respectively. The eccentricity due to stiffeners is neglected. The limit ℓ_k is the length of the stiffener in γ_1 - direction. Similarly, the bending strain energy in the j^{th} stiffener which is parallel with y_2 - line and normal to y'_1 - line (Fig. 2) is

$$U_{b,j} = \sum_{j=1}^{N_j} \frac{E_j I_j}{2} \int_0^{\ell_j} \left(\frac{\partial^2 w}{\partial y_2^2} - \frac{\partial^2 w_o}{\partial y_2^2} \right)^2_{y'_1=0} dy_2 \qquad (16)$$

The subscript j is used for j^{th} stiffener which is inclined at an angle of γ_2 with the generator of the cylinders. Where N_j denotes the number of the stiffeners in γ_2 - direction, E_j, I_j, represent Young's modulus and the moment of inertia of the j^{th} stiffener, respectively. The limit ℓ_j is the length of the stiffener in γ_2 - direction.

i. The torsion strain energy of the k^{th} and j^{th} stiffeners are

$$U_{T,k} = \sum_{k=1}^{N_k} \frac{G_k J_k}{2} \int_0^{\ell_k} \left[\frac{\partial^2 (w - w_o)}{\partial y_1 \partial y'_2} \right]^2_{y'_2=0} dy_1 \quad , \qquad (17)$$

$$U_{T,j}=\sum_{j=1}^{N_j}\frac{G_jJ_j}{2}\int_0^{l_j}\left[\frac{\partial^2(w-w_0)}{\partial y_2\,\partial y_1'}\right]^2_{y_1'=0}dy_2 \tag{18}$$

where G and J represent the shear modulus and the polar moment of inertia of stiffeners, respectively. The subscripts j is for stiffeners in γ_2 - direction and k in γ_1 - direction. In the present analysis, the inclined angles, γ_1 and γ_2, are considered in axial symmetry (i.e. $\gamma_1 = \gamma_2 = \gamma$).

CHAPTER III

INSTABILITY OF A STIFFENED CYLINDRICAL SHELL UNDER AXIAL COMPRESSION AND INTERNAL PRESSURE

3.1 Deflection Pattern and Stress Function

Let a deflection shape assume the form (12):

$$w = b_1 + b_2 \cos\frac{mx}{R} \cos\frac{ny}{R} + b_3 \cos\frac{2mx}{R} + b_4 \cos\frac{2ny}{R} \quad (19)$$

where m and n are the numbers of waves in the axial and circumferential directions, respectively. In Eq. (19), b_1 is not an independent parameter but is used to satisfy the condition of periodicity of circumferential displacement (11). It is found later to be a function of b_2, b_3 and b_4. The boundary conditions of the displacements at the ends of the stiffened cylinder are disregarded. This simplification is justified by the experimental findings of N. Nojima and S. Kanemitsu as discussed in Refs. (11) and (12). It was found that there is no appreciable length effect when the length of the cylindrical shell is greater than 1.5 times the radius of the shell. Therefore, the long stiffened cylindrical shell is considered hereon.

The corresponding stress function is

$$F = -\sigma_c \frac{y^2}{2} + \frac{pR}{t}\frac{x^2}{2} + a_{11}\cos\frac{mx}{R}\cos\frac{ny}{R} + a_{22}\cos\frac{2mx}{R}\times$$
$$\times\cos\frac{2ny}{R} + a_{02}\cos\frac{2ny}{R} + a_{20}\cos\frac{2mx}{R}$$
$$+ a_{13}\cos\frac{mx}{R}\cos\frac{3ny}{R} + a_{31}\cos\frac{3mx}{R}\cos\frac{ny}{R} \qquad (20)$$

The coefficients a_{11}, a_{22}, a_{20}, a_{02}, a_{31} and a_{13} are found in term of b_2, b_3 and b_4 from the compatibility equation (22). These coefficients are found to be:

$$\bar{a}_{20} = \frac{a_{20}}{Et^2} = (1-\Gamma)\frac{\beta}{4}\bar{b}_4 - (1-\Gamma^2)\frac{\mu^2}{32}\bar{b}_2^2$$
$$\bar{a}_{02} = \frac{a_{02}}{Et^2} = -(1-\Gamma^2)\frac{\bar{b}_2^2}{32\mu^2}$$
$$\bar{a}_{11} = \frac{a_{11}}{Et^2} = (1-\Gamma)\frac{\bar{b}_2^2\beta}{(1+\mu^2)^2} - (1-\Gamma^2)\frac{2\mu^2}{(1+\mu^2)^2}\bar{b}_2(\bar{b}_3+\bar{b}_4)$$
$$\bar{a}_{22} = \frac{a_{22}}{Et^2} = -(1-\Gamma^2)\frac{\mu^2}{(1+\mu^2)^2}\bar{b}_3\bar{b}_4$$
$$\bar{a}_{31} = \frac{a_{31}}{Et^2} = -(1-\Gamma^2)\frac{2\mu^2}{(9+\mu^2)^2}\bar{b}_2\bar{b}_4$$
$$\bar{a}_{13} = \frac{a_{13}}{Et^2} = -(1-\Gamma^2)\frac{2\mu^2}{(1+9\mu^2)^2}\bar{b}_2\bar{b}_3 \qquad (21)$$

where

$$\mu = \frac{n}{m} \qquad \beta = \frac{R}{m^2 t} \qquad \bar{b}_i = \frac{b_i}{t} \qquad i = 2, 3, 4 \qquad (22)$$

Physical considerations lead to the conclusion that the circumferential displacement, v, must be a periodic function of y. This is expressed in the condition that $\partial v/\partial y$ contains no constant terms or functions of x alone. Using the second of Eq. (1) together with Hooke's law, the following expression for $\partial v/\partial y$ can be obtained:

$$\frac{\partial v}{\partial y} = \frac{1}{E}(\sigma_y - \nu\sigma_x) - \frac{1}{2}\left(\frac{\partial w}{\partial y}\right)^2 + \frac{1}{2}\left(\frac{\partial w_o}{\partial y}\right)^2 + \left(\frac{w - w_o}{R}\right) \tag{23}$$

By substituting Eqs. (4), (19), and (20) into Eq. (23) it is found that

$$\frac{\partial v}{\partial y} = \frac{1}{E}\left(\frac{pR}{t} + \nu\sigma_c\right) - (1-\Gamma^2)\left[\frac{b_2^2}{8}\frac{n}{R} + \frac{b_3}{4}\frac{2n}{R}\right] + \frac{b_1}{R}(1-\Gamma) + \text{terms involving periodic functions} \tag{24}$$

Since v must be a periodic function of y, the constant term on the right side of Eq. (24) must be equal to zero. Thus,

$$\bar{b}_1(1-\Gamma) = (1-\Gamma^2)\frac{\mu^2}{\beta}\left(\frac{\bar{b}_2^2}{8} + \bar{b}_3^2\right) - (\bar{p} + \nu\bar{\sigma}_c) \tag{25}$$

where

$$\bar{p} = \frac{pR^2}{Et^2} \qquad \bar{\sigma}_c = \frac{\sigma_c R}{Et} \tag{26}$$

3.2 Expressions of Total Potential Energy

After substituting the expressions for w (19) and F (20) into the relations given in Chapter II, section 2.2, the various energy terms are obtained after integration. They are

$$\frac{U_e R}{\pi E t^3 L} = \bar{P}^2 + \bar{\sigma}_c^2 + 2\nu \bar{P}\bar{\sigma}_c + \bar{a}_{11}^2 \frac{(1+\mu^2)^2}{4\beta^2} + \bar{a}_{22}^2 \frac{4(1+\mu^2)^2}{\beta^2} + \frac{8}{\beta^2}(\mu^4 \bar{a}_{02}^2 + \bar{a}_{20}^2) + \frac{1}{4\beta^2}\left[(9+\mu^2)^2 \bar{a}_{31}^2 + (1+9\mu^2)^2 \bar{a}_{13}^2\right] \tag{27}$$

$$\frac{U_b R}{\pi E t^3 L} = \frac{(1-\Gamma)^2}{24(1-\nu^2)}\left[\frac{\bar{b}_2^2}{2}\cdot\frac{(1+\mu^2)^2}{\beta^2} + \frac{16}{\beta^2}(\mu^4 \bar{b}_3^2 + \bar{b}_4^2)\right] \tag{28}$$

$$\frac{U_c R}{\pi E t^3 L} = -2\left[\bar{\sigma}_c^2 + \nu \bar{P}\bar{\sigma}_c + \left(\frac{\bar{\sigma}_c}{8\beta}\bar{b}_2^2 + \frac{\bar{\sigma}_c}{\beta}\bar{b}_4^2\right)(1-\Gamma^2)\right] \tag{29}$$

$$\frac{U_p R}{\pi E t^3 L} = 2\bar{P}(1-\Gamma^2)\frac{\mu^2}{\beta}\left(\frac{\bar{b}_2^2}{8} + \bar{b}_3^2\right) - (\bar{P} + \nu\bar{\sigma}_c) \tag{30}$$

$$\frac{U_{b,k} R}{\pi E t^3 L} = \frac{(1-\Gamma)^2}{\beta^2}\sum_{k=1}^{N_k}\frac{\bar{E}_k \bar{I}_k \bar{\ell}_k}{8}\left[\bar{b}_2^2\left(C_1^4 + C_2^4 + 6\mu^2 C_1^2 C_2^2\right) + 32\left(\bar{b}_3^2 \mu^4 C_2^4 + \bar{b}_4^2 C_1^4\right)\right] + R_1 \tag{31}$$

$$\frac{U_{b,j}R}{\pi E t^3 L} = \frac{(1-\Gamma)^2}{\beta^2} \sum_{j=1}^{N_j} \frac{\bar{E}_j \bar{I}_j \bar{l}_j}{8} \left[\bar{b}_2^{-2} \left(C_3^4 + C_4^4 + 6\mu^2 C_3^2 C_4^2 \right) + 32 \left(\bar{b}_3^{-2} \mu^4 C_4^4 + \bar{b}_4^{-2} C_3^4 \right) \right] + R_2 \tag{32}$$

$$\frac{U_{T,k}R}{\pi E t^3 L} = \frac{(1-\Gamma)^2}{\beta^2} \sum_{k=1}^{N_k} \frac{\bar{G}_k \bar{J}_k \bar{l}_k}{16} \left\{ \bar{b}_2^{-2} \left[(C_1+\mu C_2)^2 (C_2-\mu C_1)^2 + (C_1-\mu C_2)^2 (C_2+\mu C_1)^2 \right] + 64 C_1^2 C_2^2 \left(\bar{b}_4^{-2} + \bar{b}_3^{-2} \mu^4 \right) \right\} + R_3 \tag{33}$$

$$\frac{U_{T,j}R}{\pi E t^3 L} = \frac{(1-\Gamma)^2}{\beta^2} \sum_{j=1}^{N_j} \frac{\bar{G}_j \bar{J}_j \bar{l}_j}{16} \left\{ \bar{b}_2^{-2} \left[(C_3+\mu C_4)^2 (C_4-\mu C_3)^2 + (C_3-\mu C_4)^2 (C_4+\mu C_3)^2 \right] + 64 C_3^2 C_4^2 \left(\bar{b}_4^{-2} + \bar{b}_3^{-2} \mu^4 \right) \right\} + R_4 \tag{34}$$

where

$$\bar{E}_k = \frac{E_k}{E} \quad , \quad \bar{I}_k = \frac{I_k}{\pi R t^3} \quad , \quad \bar{G}_k = \frac{G_k}{E} \quad , \quad \bar{J}_k = \frac{J_k}{\pi R t^3}$$

$$\bar{E}_j = \frac{E_j}{E} \quad , \quad \bar{I}_j = \frac{I_j}{\pi R t^3} \quad , \quad \bar{G}_j = \frac{G_j}{E} \quad , \quad \bar{J}_j = \frac{J_j}{\pi R t^3}$$

$$\bar{l}_k = \frac{l_k}{L} \quad , \quad C_1 = \cos\gamma_1 \quad , \quad C_2 = \sin\gamma_1$$

$$\bar{l}_j = \frac{l_j}{L} \quad , \quad C_3 = \cos\gamma_2 \quad , \quad C_4 = \sin\gamma_2 \tag{35}$$

The expressions R_1, R_2, R_3, and R_4 are very lengthy and can be neglected if the stiffeners are located uniformly and not far apart. They are listed and discussed in Appendix A.

The total potential of the system is the sum of the strain energies and the potential of the applied loads, as follows:

$$U_1 = U_e + U_b + U_c + U_p + U_{b,k} + U_{b,j} + U_{T,k} + U_{T,j} \tag{36}$$

In nondimensional form:

$$\bar{U}_1 = \frac{U_1 R}{\pi E t^3 L} = \bar{p}^2 - \bar{\sigma}_c^2 + (1-\Gamma^2)\bar{p}\frac{2\mu^2}{\beta}\left(\frac{\bar{b}_2^2}{8} + \bar{b}_3^2\right)$$
$$-2(\bar{p} + \nu\bar{\sigma}_c) - \frac{2\bar{\sigma}_c}{\beta}(1-\Gamma^2)\left(\frac{\bar{b}_2^2}{8} + \bar{b}_4^2\right) + \bar{a}_{11}^2\frac{(1+\mu^2)^2}{4\beta^2}$$
$$+ \bar{a}_{22}^2\frac{4(1+\mu^2)^2}{\beta^2} + \frac{8}{\beta^2}\left(\bar{a}_{02}^2\mu^4 + \bar{a}_{20}^2\right) + \frac{1}{4\beta^2}\left[(9+\mu^2)^2\bar{a}_{31}^2\right.$$
$$\left. + (1+9\mu^2)^2\bar{a}_{13}^2\right] + \frac{(1-\Gamma)^2}{24(1-\nu^2)\beta^2}\left[\frac{\bar{b}_2^2}{2}(1+\mu^2)^2 + 16\left(\mu^4\bar{b}_3^2 + \bar{b}_4^2\right)\right]$$

$$+\frac{(1-\Gamma)^2}{\beta^2}\Bigg[\sum_{k=1}^{N_k}\bar{E}_k\bar{I}_k\bar{l}_k\Bigg\{\bar{b}_2^2\,\frac{C_1^4+6\mu^2C_1^2C_2^2+C_2^4\mu^4}{8}+4\left(\bar{b}_3^2\mu^4C_2^4+\bar{b}_4^2C_1^4\right)\Bigg\}$$

$$+\sum_{j=1}^{N_j}\bar{E}_j\bar{I}_j\bar{l}_j\Bigg\{\frac{\bar{b}_2^2}{8}\left(C_3^4+6\mu^2C_3^2C_4^2+\mu^4C_4^4\right)+4\left(\bar{b}_3^2\mu^4C_4^4+\bar{b}_4^2C_3^4\right)\Bigg\}$$

$$+\sum_{k=1}^{N_k}\bar{G}_k\bar{J}_k\bar{l}_k\Bigg\{\frac{\bar{b}_2^2}{16}\left[(C_1+\mu C_2)^2(C_2-\mu C_1)^2+(C_1-\mu C_2)^2(C_2+\mu C_1)^2\right]$$

$$+4C_1^2C_2^2\left(\bar{b}_3^2\mu^4+\bar{b}_4^2\right)\Bigg\}+\sum_{j=1}^{N_j}\bar{G}_j\bar{J}_j\bar{l}_j\Bigg\{\frac{\bar{b}_2^2}{16}\Big[(C_3+\mu C_4)^2(C_4-\mu C_3)^2$$

$$+(C_3-\mu C_4)^2(C_4+\mu C_3)^2\Big]+4C_3^2C_4^2\left(\bar{b}_3^2\mu^4+\bar{b}_4^2\right)\Bigg\}\Bigg]$$

$$+R_1+R_2+R_3+R_4 \qquad (37)$$

3.3 Minimization of Total Potential Energy

The variation of the total potential with respect to each of the arbitrary parameters must vanish for equilibrium, this yields

$$\frac{\partial\bar{\bar{U}}_1}{\partial\bar{b}_2}=0\,,\quad\frac{\partial\bar{\bar{U}}_1}{\partial\bar{b}_3}=0\,,\quad\frac{\partial\bar{\bar{U}}_1}{\partial\bar{b}_4}=0 \qquad (38)$$

After differentiation, the following three equations are established:

$$\frac{1}{1-\Gamma}(\bar{\sigma}_c-\mu^2\bar{p})=\frac{1}{\beta}\left\{\frac{(1+\mu^2)^2}{12(1-\nu^2)}+\sum_{k=1}^{N_k}\frac{\bar{E}_k\bar{I}_k\bar{l}_k}{2}(C_1^4+6\mu^2C_1^2C_2^2+\mu^4C_2^4)\right.$$
$$+\sum_{j=1}^{N_j}\frac{\bar{E}_j\bar{I}_j\bar{l}_j}{2}(C_3^4+6\mu^2C_3^2C_4^2+C_4^4\mu^4)$$
$$+\sum_{k=1}^{N_k}\frac{\bar{G}_k\bar{J}_k\bar{l}_k}{4}\left[(C_1+\mu C_2)^2(C_2-\mu C_1)^2+(C_1-\mu C_2)^2(C_2+\mu C_1)^2\right]$$
$$\left.+\sum_{j=1}^{N_j}\frac{\bar{G}_j\bar{J}_j\bar{l}_j}{4}\left[(C_3+\mu C_4)^2(C_4-\mu C_3)^2+(C_3-\mu C_4)^2(C_4+\mu C_3)^2\right]\right\}$$
$$+\frac{\beta}{(1+\mu^2)^2}-\left[\frac{2(2+\Gamma)(\bar{b}_3+\bar{b}_4)}{(1+\mu^2)^2}+\frac{\bar{b}_4}{2}\right]\mu^2+\frac{4\mu^4(\bar{b}_3+\bar{b}_4)^2(1+\Gamma)}{\beta(1+\mu^2)^2}$$
$$+\frac{\bar{b}_2^2(1+\mu^4)(1+\Gamma)}{16\beta}+\frac{4\mu^4(1+\Gamma)}{\beta}\left[\frac{\bar{b}_3^2}{(1+9\mu^2)^2}+\frac{\bar{b}_4^2}{(9+\mu^2)^2}\right] \tag{39}$$

$$-\frac{\mu^2\bar{p}}{(1-\Gamma)}=\frac{\mu^2}{4(1+\mu^2)}\cdot\frac{\bar{b}_2^2}{\bar{b}_3}+\frac{\bar{b}_2}{\beta}\left(1+\frac{\bar{b}_4}{\bar{b}_3}\right)\frac{\mu^4(1+\Gamma)}{2(1+\mu^2)^2}+\frac{\bar{b}_4^2}{\beta}\cdot\frac{2\mu^4(1+\Gamma)}{(1+\mu^2)^2}$$
$$+\frac{\bar{b}_2^2}{\beta}\frac{\mu^4(1+\Gamma)}{2(1+9\mu^2)^2}+\frac{1}{\beta}\left\{\frac{\mu^4}{3(1-\nu^2)}+2\left[\sum_{k=1}^{N_k}\bar{E}_k\bar{I}_k\bar{l}_kC_2^4\mu^4\right.\right.$$
$$\left.\left.+\sum_{j=1}^{N_j}\bar{E}_j\bar{I}_j\bar{l}_jC_4^4\mu^4+\sum_{k=1}^{N_k}\bar{G}_k\bar{J}_k\bar{l}_kC_1^2C_2^2\mu^4+\sum_{j=1}^{N_j}\bar{G}_j\bar{J}_j\bar{l}_jC_3^2C_4^2\mu^4\right]\right\} \tag{40}$$

$$\frac{\bar{\sigma}_c}{1-\Gamma}=-\frac{\bar{b}_2^2}{\bar{b}_4}\frac{\mu^2}{4(1+\mu^2)^2}+\frac{\bar{b}_2^2}{\beta}\cdot\frac{\mu^4(1+\Gamma)}{2(1+\mu^2)^2}\left(1+\frac{\bar{b}_3}{\bar{b}_4}\right)+\frac{\bar{b}_3^2}{\beta}\frac{2\mu^4(1+\Gamma)}{(1+\mu^2)^2}+$$

$$+\frac{\beta}{4}-(1+\Gamma)\frac{\bar{b}_2^2}{\bar{b}_4}\frac{\mu^2}{32}+(1+\Gamma)\frac{\bar{b}_2^2\mu^4}{\beta\,2(9+\mu^2)^2}+\frac{1}{\beta}\left\{\frac{1}{3(1-\nu^2)}\right.$$
$$\left.+2\left[\sum_{k=1}^{N_k}\bar{E}_k\bar{I}_k\bar{l}_k C_1^4+\sum_{j=1}^{N_j}\bar{E}_j\bar{I}_j\bar{l}_j C_3^4+\sum_{k=1}^{N_k}\bar{G}_k\bar{J}_k\bar{l}_k C_1^2C_2^2\right.\right.$$
$$\left.\left.+\sum_{j=1}^{N_j}\bar{G}_j\bar{J}_j\bar{l}_j C_3^2C_4^2\right]\right\} \qquad (41)$$

For brevity, Eqs. (39), (40) and (41) may be rewritten as:

$$\phi_1\frac{\beta}{1-\Gamma}=A_1+\beta^2(A_2+A_3\eta+A_4\eta^2)+\bar{b}_2^2A_5 \qquad (42)$$

$$\phi_2\frac{\beta}{1-\Gamma}=B_1+\beta^2B_4\eta^2+\bar{b}_2^2\left(B_5+\frac{B_6}{\eta}\right) \qquad (43)$$

$$\phi_3\frac{\beta}{1-\Gamma}=H_1+\beta^2(H_2+H_4\eta^2)+\bar{b}_2^2\left(H_5+\frac{H_6}{\eta}\right) \qquad (44)$$

where

$$\phi_1 = \bar{\sigma}_c-\mu^2\bar{p}$$
$$A_1 = \frac{(1+\mu^2)^2}{12(1-\nu^2)}+S_1$$
$$A_2 = \frac{1}{(1+\mu^2)^2}$$
$$A_3 = -\left[\frac{2(2+\Gamma)(1+\eta_1)}{(1+\mu^2)^2}+\frac{\eta_1}{2}\right]\mu^2$$

$$A_4 = 4(1+\Gamma)\,\mu^4 \left[\frac{(1+\eta_1)^2}{(1+\mu^2)} + \frac{\eta_1^2}{(9+\mu^2)^2} + \frac{1}{(1+9\mu^2)^2}\right]$$

$$A_5 = (1+\Gamma)\,\frac{1+\mu^4}{16}$$

$$\begin{aligned} S_1 = &\sum_{k=1}^{N_k} \frac{\bar{E}_k \bar{I}_k \bar{l}_k}{2}\left(C_1^4 + 6\mu^2 C_1^2 C_2^2 + \mu^4 C_2^4\right) \\ &+ \sum_{j=1}^{N_j} \frac{\bar{E}_j \bar{I}_j \bar{l}_j}{2}\left(C_3^4 + 6\mu^2 C_3^2 C_4^2 + \mu^4 C_4^4\right) \\ &+ \sum_{k=1}^{N_k} \frac{\bar{E}_k \bar{I}_k \bar{l}_k}{4}\left[(C_1+\mu C_2)^2 (C_2-\mu C_1)^2 + (C_1-\mu C_2)^2 (C_2+\mu C_1)^2\right] \\ &+ \sum_{j=1}^{N_j} \frac{\bar{E}_j \bar{I}_j \bar{l}_j}{4}\left[(C_3+\mu C_4)^2 (C_4-\mu C_3)^2 + (C_3-\mu C_4)^2 (C_4+\mu C_3)^2\right] \end{aligned} \qquad (45)$$

$$\phi_2 = -\mu^2 \bar{p}$$

$$B_1 = \frac{\mu^4}{3(1-\nu^2)} + S_2$$

$$B_4 = (1+\Gamma)\frac{2\mu^4}{(1+\mu^2)^2}\eta_1^2$$

$$B_5 = (1+\Gamma)\left[\frac{1}{(1+9\mu^2)^2} + \frac{(1+\eta_1)}{(1+\mu^2)^2}\right]\frac{\mu^4}{2}$$

$$B_6 = -\frac{\mu^2}{4(1+\mu^2)^2}$$

$$\begin{aligned} S_2 = &\sum_{k=1}^{N_k} \bar{E}_k \bar{I}_k \bar{l}_k C_2^4 \mu^4 + \sum_{j=1}^{N_j} \bar{E}_j \bar{I}_j \bar{l}_j C_4^4 \mu^4 \\ &+ \sum_{k=1}^{N_k} \bar{G}_k \bar{J}_k \bar{l}_k C_1^2 C_2^2 \mu^4 + \sum_{j=1}^{N_j} \bar{G}_j \bar{J}_j \bar{l}_j C_3^2 C_4^2 \mu^4 \end{aligned}$$

(46)

$$\phi_3 = \bar{\sigma}_c$$

$$H_1 = \frac{1}{3(1-\nu^2)} + S_3$$

$$H_2 = \frac{1}{4}$$

$$H_4 = (1+\Gamma)\frac{2\mu^4}{(1+\mu^2)^2}$$

$$H_5 = (1+\Gamma)\frac{\mu^4}{2}\left[\frac{1}{(1+\mu^2)^2} + \left(1+\frac{1}{\eta_1}\right)\frac{1}{(1+\mu^2)^2}\right]$$

$$H_6 = -\left[\frac{1}{(1+\mu^2)^2} + \frac{1+\Gamma}{8}\right]\frac{\mu^2}{4\eta_1}$$

$$S_3 = \sum_{k=1}^{N_k} \bar{E}_k \bar{I}_k \bar{l}_k C_1^4 + \sum_{j=1}^{N_j} \bar{E}_j \bar{I}_j \bar{l}_j C_3^4 + \sum_{k=1}^{N_k} \bar{G}_k \bar{J}_k \bar{l}_k C_1^2 C_2^2 + \sum_{j=1}^{N_j} \bar{E}_j \bar{I}_j \bar{l}_j C_3^2 C_4^2 \qquad (47)$$

$$\eta = \frac{\bar{b}_3}{\beta} \qquad \eta_1 = \frac{\bar{b}_4}{\bar{b}_3} \qquad (48)$$

Eliminating $\bar{b}_2$ and β from Eqs. (42), (43), (44), the following equation is obtained:

$$M_1 \bar{\sigma}_c^2 + M_2 \bar{\sigma}_c + M_3 = 0 \qquad (49)$$

where

$$M_1 = \frac{1}{(1-\Gamma^2)}\left[\frac{D_2 D_3}{F^2}\left(H_5+\frac{H_6}{\eta}-A_5\right)^2+\frac{F_2}{F_3}\left(B_5+\frac{B_6}{\eta}\right)^2 - \left(\frac{F_2 D_3}{F_3^2}+\frac{D_2}{F_3}\right)\left(H_5+\frac{H_6}{\eta}-A_5\right)\left(B_5+\frac{B_6}{\eta}\right)\right]$$

$$M_2 = -\frac{\bar{\rho}\mu^2}{(1-\Gamma^2)}\left\{\frac{2D_2 D_3}{F_3^2}\left(H_5+\frac{H_6}{\eta}\right)\left(H_5+\frac{H_6}{\eta}-A_5\right) + \frac{2F_2}{F_3}\left(B_5+\frac{B_6}{\eta}-A_5\right)-\left(\frac{F_2 D_3}{F_3^2}+\frac{D_2}{F_3}\right)\left[2\left(B_5+\frac{B_6}{\eta}\right)\times \left(H_5+\frac{H_6}{\eta}\right)+A_5^2-A_5\left(B_5+\frac{B_6}{\eta}+H_5+\frac{H_6}{\eta}\right)\right]\right\}$$

$$M_3 = \frac{\bar{\rho}\mu^4}{(1-\Gamma^2)}\left[\frac{D_2 D_3}{F_3^2}\left(H_5+\frac{H_6}{\eta}\right)^2+\frac{F_2}{F_3}\left(B_5+\frac{B_6}{\eta}-A_5\right)^2 - \left(\frac{F_2 D_3}{F_3^2}+\frac{D_2}{F_3}\right)\left(H_5+\frac{H_6}{\eta}\right)\left(B_5+\frac{B_6}{\eta}-A_5\right)\right] + \frac{D_3^2 F_2^2}{F_3^2}-\frac{2D_2 D_3 F_2}{F_3}+D_2^2$$

(50)

$$D_2 = A_1\left(B_5+\frac{B_6}{\eta}\right)-B_1 A_5$$

$$D_3 = \left(A_2+A_3\eta+A_4\eta^2\right)\left(B_5+\frac{B_6}{\eta}\right)-B_4 A_5\eta^2$$

(51)

$$F_2 = A_1\left(H_5 + \frac{H_6}{\eta}\right) - H_1 A_5$$

$$F_3 = \left(A_2 + A_3\eta + A_4\eta^2\right)\left(H_5 + \frac{H_6}{\eta}\right) - \left(H_2 + H_4\eta^2\right) A_5 \qquad (52)$$

Equation (49) is the governing equation for the stationary load of a stiffened shell under axial compression.

The numerical calculations have been carried out on the IBM 709 and the computer program used is attached as Appendix B.

CHAPTER IV

INSTABILITY OF A STIFFENED CYLINDRICAL SHELL UNDER BENDING AND INTERNAL PRESSURE

4.1 Deflection Pattern and Approximate Stress Function

When a cylindrical shell is subjected to either pure bending or eccentrically applied compression, an approximate form of the deflection pattern is assumed (14):

$$w = b_1 + \cos^2\left(\frac{y}{2R}\right)\left(b_2 \cos\frac{mx}{R}\cos\frac{ny}{R} + b_3\cos\frac{2mx}{R} + b_4\cos\frac{2ny}{R}\right) \tag{53}$$

This approximate deflection pattern is obtained by multiplying the pattern of the axial compression by $\cos^2(y/2R)$ which signifies the localized buckling on one side of the stiffened shells. The effects of the end restraints are also neglected.

The corresponding stress function F is proposed

$$F = -\frac{\sigma}{2}y^2 + \sigma_b R^2 \cos\frac{y}{R} + \frac{1}{2}\frac{pR}{t}x^2 + a_{11}\cos\frac{mx}{R}\cos\frac{ny}{R}$$
$$+ a_{22}\cos\frac{2mx}{R}\cos\frac{2ny}{R} + a_{20}\cos\frac{2mx}{R} + a_{02}\cos\frac{2ny}{R}$$
$$+ a_{31}\cos\frac{3mx}{R}\cos\frac{ny}{R} + a_{13}\cos\frac{mx}{R}\cos\frac{3ny}{R} \qquad (54)$$

The stresses σ and σ_b are the average axial compression and peak bending stress, respectively, and are positive for compression.

The coefficients a_{20}, a_{02}, a_{11}, a_{22}, a_{31} and a_{13} in Eq. (54) can be expressed in terms of b_2, b_3 and b_4 by the Galerkin method. This method establishes the following set of equations:

$$\int_0^L \int_0^{2\pi R} Q_1 \cos\frac{mx}{R}\cos\frac{ny}{R}\,dy\,dx = 0$$
$$\int_0^L \int_0^{2\pi R} Q_1 \cos\frac{2mx}{R}\cos\frac{2ny}{R}\,dy\,dx = 0$$
$$\int_0^L \int_0^{2\pi R} Q_1 \cos\frac{2mx}{R}\,dy\,dx = 0$$
$$\int_0^L \int_0^{2\pi R} Q_1 \cos\frac{2ny}{R}\,dy\,dx = 0$$
$$\int_0^L \int_0^{2\pi R} Q_1 \cos\frac{mx}{R}\cos\frac{3ny}{R}\,dy\,dx = 0$$
$$\int_0^L \int_0^{2\pi R} Q_1 \cos\frac{3mx}{R}\cos\frac{ny}{R}\,dy\,dx = 0 \qquad (55)$$

where

$$Q_1 = \nabla^4 F - E\left[\left(\frac{\partial^2 w}{\partial x \partial y}\right)^2 - \frac{\partial^2 w}{\partial x^2}\frac{\partial^2 w}{\partial y^2} + \frac{\partial^2 w_0}{\partial x^2}\frac{\partial^2 w_0}{\partial y^2} - \left(\frac{\partial^2 w_0}{\partial x \partial y}\right)^2 - \frac{1}{R}\frac{\partial^2 w}{\partial x^2} + \frac{1}{R}\cdot\frac{\partial^2 w_0}{\partial x^2}\right] \tag{56}$$

After the expressions for w in Eq. (53) and F in Eq. (54) are substituted in Eq. (55) and the integration carried out, the following relations are found:

$$\begin{aligned}
\bar{a}_{20} &= \frac{a_{20}}{Et^2} = \frac{1}{16}\left[(1-\Gamma)\,2\,\bar{b}_4\beta - \left(\frac{3}{16}\mu^2 + \frac{1}{16m^2}\right)\bar{b}_2^2(1-\Gamma^2)\right] \\
\bar{a}_{02} &= \frac{a_{02}}{Et^2} = -(1-\Gamma^2)\frac{3\bar{b}_2^2}{256\mu^2} \\
\bar{a}_{11} &= \frac{a_{11}}{Et^2} = -\frac{(1-\Gamma^2)\left[\left(\frac{3\mu^2}{2} + \frac{1}{8m^2}\right)(\bar{b}_3+\bar{b}_4)\bar{b}_2\right] - (1-\Gamma)\beta\,\bar{b}_2}{2(1+\mu^2)^2} \\
\bar{a}_{22} &= \frac{a_{22}}{Et^2} = -(1-\Gamma^2)\frac{\frac{\bar{b}_2^2}{16m^2} + \bar{b}_3\bar{b}_4\left(6\mu^2 + \frac{1}{2m^2}\right)}{16(1+\mu^2)^2} \\
\bar{a}_{31} &= \frac{a_{31}}{Et^2} = -\frac{\left(3\mu^2 + \frac{9}{4m^2}\right)}{4(9+\mu^2)^2}\,\bar{b}_2\bar{b}_4(1-\Gamma^2) \\
\bar{a}_{13} &= \frac{a_{13}}{Et^2} = -(1-\Gamma^2)\,\bar{b}_2\bar{b}_3\,\frac{3\mu^2 + \frac{1}{4m^2}}{4(9\mu^2+1)^2}
\end{aligned} \tag{57}$$

where Γ, μ, β and $\bar{b}_i$ are same as given in Eqs. (6) and (22), respectively.

In order to find the b_1 as a function of b_2, b_3 and b_4, we derive as in section 3.1 the relation:

$$\bar{b}_1(1-\Gamma) = -(\bar{p}+\nu\bar{\sigma}) + \frac{1-\Gamma^2}{4\beta}\left[\frac{\bar{b}_2^2\mu^2}{8} + \frac{\bar{b}_2^2}{16}\left(\mu^2+\frac{1}{m^2}\right) + \bar{b}_3^2\mu^2 + \frac{\bar{b}_3^2}{4}\left(2\mu^2+\frac{1}{2m^2}\right) + \frac{\bar{b}_4^2}{8m^2}\right]$$

(58)

4.2 Expressions of Total Potential Energy

The total potential of the system is the sum of the strain energies and the potential of the applied loads. By adding the Eqs. (8), (9), (10), (11), (12), (15), (16), (17) and (18), the total potential may be expressed as follows:

$$U_2 = U_e + U_b + U_m + U_c + U_p + U_{b,k} + U_{b,j} + U_{T,k} + U_{T,j}$$

(59)

If w, F and $\bar{b}_1$ as given by Eqs. (53), (54) and (58) respectively are substituted in Eq. (59) and the integration carried out, the total potential is obtained in the following form:

$$\bar{U}_2 = \frac{U_2 R}{\pi E L t^3} = -\bar{p}^2 - \bar{\sigma}^2 - \frac{\bar{\sigma}_b^2}{2} - 2\nu\bar{p}\bar{\sigma} - \frac{\bar{b}_2^2}{\beta}\frac{3(1-\Gamma^2)}{32}\bar{\sigma} - \bar{b}_4^2\frac{3(1-\Gamma^2)}{4\beta}\bar{\sigma} - (1-\Gamma^2)\left(\frac{\bar{b}_2^2}{16}+\frac{\bar{b}_4^2}{2}\right)\frac{\bar{\sigma}_b}{\beta} +$$

$$+(1-\Gamma^2)\frac{\bar{p}}{2\beta}\Big[\bar{b}_2^2\frac{\mu^2}{8}+\frac{\bar{b}_2^2}{16}\Big(\mu^2+\frac{1}{m^2}\Big)+\bar{b}_3^2\mu^2+\frac{\bar{b}_3^2}{4}\Big(2\mu^2+\frac{1}{2m^2}\Big)$$

$$+\bar{b}_4^2\frac{1}{8m^2}\Big]+\sum_{k=1}^{N_R}\frac{\bar{E}_k\bar{I}_k\bar{l}_k}{16\beta^2}\Big\{\frac{\bar{b}_2^2}{2}\Big[\frac{3}{2}\Big(C_1^4+6\mu^2C_1^2C_2^2+\mu^4C_2^4\Big)$$

$$+\frac{C_2^4}{2}\Big(\frac{1}{m^4}+\frac{6\mu^2}{m^2}\Big)+\frac{3C_1^2C_2^2}{m^2}\Big]+\bar{b}_3^2\frac{C_2^4}{2}\Big[48\mu^4+24\frac{\mu^2}{m^2}+\frac{1}{m^4}\Big]$$

$$+\frac{\bar{b}_4^2}{2}\Big[48C_1^4+24\frac{C_1^2C_2^2}{m^2}+\frac{C_2^4}{m^4}\Big]\Big\}+\sum_{j=1}^{N_j}\frac{\bar{E}_j\bar{I}_j\bar{l}_j}{16\beta^2}\Big\{\frac{\bar{b}_2^2}{2}\Big[\frac{3}{2}\Big(C_3^4$$

$$+6\mu^2C_3^2C_4^2+\mu^4C_4^4\Big)+\frac{C_4^4}{2}\Big(\frac{6\mu^2}{m^2}+\frac{1}{m^4}\Big)+\frac{3C_3^2C_4^2}{m^2}\Big]+\frac{\bar{b}_3^2C_4^4}{2}\Big[\frac{1}{m^4}$$

$$+\frac{24\mu^2}{m^2}+48\mu^4\Big]+\frac{\bar{b}_4^2}{2}\Big(\frac{C_4^4}{m^4}+\frac{24C_3^2C_4^2}{m^2}+48C_3^4\Big)\Big]\Big\}$$

$$+\sum_{k=1}^{N_R}\frac{\bar{G}_k\bar{J}_k\bar{l}_k}{16\beta^2}\Big\{\frac{\bar{b}_2^2}{2}\Big[\frac{3}{4}\Big[(C_1+\mu C_2)^2(C_2-\mu C_1)^2+(C_1-\mu C_2)^2(C_2+\mu C_1)^2\Big]$$

$$+\frac{1}{2m^2}\Big[(C_1^2+\mu^2C_2^2)\cdot C_1^2-4(1-\mu^2)C_1^2C_2^2+(C_2^2+\mu^2C_1^2)C_2^2\Big]+\frac{C_1^2C_2^2}{2m^4}\Big]$$

$$+16\bar{b}_3^2\Big(\frac{3}{2}\mu^4+\frac{3\mu^2}{4m^2}+\frac{1}{32m^4}\Big)C_1^2C_2^2+16\bar{b}_4^2\Big[\Big(\frac{3}{2}-\frac{1}{2m^2}$$

$$+\frac{1}{32m^4}\Big)C_1^2C_2^2+\frac{C_1^4+C_2^4}{8m^2}\Big]\Big\}+\bar{a}_{11}^2\frac{(1+\mu)^2}{4\beta^2}+\bar{a}_{22}^2\frac{4(1+\mu^2)^2}{\beta^2}$$

$$+\bar{a}_{20}^2\frac{8}{\beta^2}+\bar{a}_{02}^2\frac{8\mu^4}{\beta^2}+\bar{a}_{31}^2\frac{(9+\mu^2)^2}{4\beta^2}+\bar{a}_{13}^2\frac{(1+9\mu^2)^2}{4\beta^2}$$

$$+\frac{(1-\Gamma)^2}{192\beta^2(1-\nu^2)}\Big\{\bar{b}_2^2(1+\mu^2)^2+\frac{\bar{b}_2^2}{2}\Big[(1+\mu^2)^2+\frac{6\mu^2}{m^2}+\frac{2}{m^2}+\frac{1}{m^4}\Big]+\bar{b}_4^2\Big(48+\frac{8}{m^2}+\frac{1}{m^4}\Big)+$$

$$+\bar{b}_3^2\left(48\mu^4+24\frac{\mu^2}{m^2}+\frac{1}{m^4}\right)\Big\}+\sum_{j=1}^{N_j}\frac{\bar{G}_j\bar{J}_j\bar{l}_j}{16\beta^2}\Big\{\frac{\bar{b}_2^2}{2}\Big[\frac{3}{4}\Big[(C_3+\mu C_4)^2\times$$

$$\times(C_4-\mu C_3)^2+(C_3-\mu C_4)^2(C_4+\mu C_3)^2\Big]+\frac{1}{2m^2}\Big[(C_3^2+\mu^2C_4^2)C_3^2$$

$$-4(1-\mu^2)C_3^2C_4^2+(C_4^2+\mu^2C_3^2)C_4^2\Big]+\frac{C_3^2C_4^2}{2m^4}\Big]+16\bar{b}_2^2\Big(\frac{3}{2}\mu^4$$

$$+\frac{3\mu^2}{4m^2}+\frac{1}{32m^4}\Big)C_3^2C_4^2+16\bar{b}_4^2\Big[\Big(\frac{3}{2}-\frac{1}{2m^2}+\frac{1}{32m^4}\Big)C_3^2C_4^2$$

$$+\frac{C_3^4+C_4^4}{8m^2}\Big]\Big\}+\bar{R}_1+\bar{R}_2+\bar{R}_3+\bar{R}_4$$

(60)

where $\bar{R}_1$, $\bar{R}_2$, $\bar{R}_3$, $\bar{R}_4$ are also the portion of the energy of the stiffeners which have the similar expressions as R_1, R_2, R_3 and R_4. Since they are neglected in the numerical calculation, their detailed expressions will not be elaborated here. From the discussion in Ref. (14) it is indicated that m has a greater magnitude when R/t is greater. In the present analysis, we are concerned only with extremely thin shells; hence this ratio is large. Therefore, for practical purposes $1/m^2$ and $1/m^4$ are negligible compared to unity. Thus, from Eq. (60), the total potential can be simplified as follows:

$$\overline{U_2} = -\bar{p}^2 - \bar{\sigma}^2 - \frac{1}{2}\bar{\sigma}_b^2 - 2\nu\bar{\sigma}\bar{p} - (1-\Gamma^2)\frac{\bar{b}_2^2}{\beta}\frac{3\bar{\sigma}}{32} - (1-\Gamma^2)\frac{\bar{b}_4^2}{\beta}\frac{3\bar{\sigma}}{4}$$

$$+(1-\Gamma^2)\frac{\bar{p}}{2\beta}\left(\frac{\bar{b}_2^2}{8}+\bar{b}_3^2\right)\frac{3\mu^2}{2} - (1-\Gamma^2)\frac{\bar{\sigma}_b}{2\beta}\left(\bar{b}_4^2+\frac{\bar{b}_3^2}{8}\right)$$

$$+\tilde{a}_{11}^2\frac{(1+\mu^2)^2}{4\beta^2}+\tilde{a}_{22}^2\frac{4(1+\mu^2)^2}{\beta^2}+\tilde{a}_{20}^2\frac{8}{\beta^2}+\tilde{a}_{02}^2\frac{8\mu^4}{\beta^2}$$

$$+\tilde{a}_{31}^2\frac{(9+\mu^2)^2}{4\beta^2}+\tilde{a}_{13}^2\frac{(1+9\mu^2)^2}{4\beta^2}+\sum_{k=1}^{N_k}\frac{\bar{E}_k\bar{I}_k\bar{l}_k}{16\beta^2}\left[\frac{3}{4}\bar{b}_2^2(C_1^4+C_2^4\mu^4\right.$$

$$\left.+6\mu^2C_1^2C_2^2)+24\bar{b}_3^2\mu^4C_2^4+24\bar{b}_4^2C_1^4\right]+\sum_{j=1}^{N_j}\frac{\bar{E}_j\bar{I}_j\bar{l}_j}{16\beta^2}\left[\frac{3\bar{b}_2^2}{4}(C_3^4\right.$$

$$\left.+\mu^4C_4^4+6\mu^2C_3^2C_4^2)+24\bar{b}_3^2\mu^4C_4^4+24\bar{b}_4^2C_3^4\right]+\sum_{k=1}^{N_k}\frac{\bar{G}_k\bar{J}_k\bar{l}_k}{16\beta^2}\times$$

$$\times\left\{\frac{3}{8}\bar{b}_2^2\left[(C_1+\mu C_2)^2(C_2-\mu C_1)^2+(C_1-\mu C_2)^2(C_2+\mu C_1)^2\right]+24\bar{b}_3^2\mu^4C_1^2C_2^2\right.$$

$$\left.+24\bar{b}_4^2C_1^2C_2^2\right\}+\sum_{j=1}^{N_j}\frac{\bar{G}_j\bar{J}_j\bar{l}_j}{16\beta^2}\left\{\frac{3}{8}\bar{b}_2^2\left[(C_3+\mu C_4)^2(C_4-\mu C_3)^2\right.\right.$$

$$\left.\left.+(C_3-\mu C_4)^2(C_4+\mu C_3)^2\right]+24\bar{b}_3^2\mu^4C_3^2C_4^2+24\bar{b}_4^2C_3^2C_4^2\right\}$$

$$+\frac{(1-\Gamma)^2}{192\beta^2(1-\nu^2)}\left[\frac{3}{2}\bar{b}_2^2(1+\mu^2)^2+48(\bar{b}_4^2+\mu^4\bar{b}_3^2)\right] \qquad (61)$$

where

$$\tilde{a}_{20}=\frac{1}{16}\left[2(1-\Gamma)\bar{b}_4\beta-(1-\Gamma^2)\bar{b}_2^2\frac{3\mu^2}{16}\right]$$

$$\tilde{a}_{02} = -(1-\Gamma^2)\frac{3\bar{b}_2^2}{256\mu^2}$$

$$\tilde{a}_{11} = -\frac{(1-\Gamma^2)\left[\frac{3\mu^2}{2}(\bar{b}_3+\bar{b}_4)\bar{b}_2\right]-(1-\Gamma)\beta\bar{b}_2}{2(1+\mu^2)^2}$$

$$\tilde{a}_{22} = (1-\Gamma^2)\frac{3\mu^2}{8(1+\mu^2)^2}\bar{b}_3\bar{b}_4$$

$$\tilde{a}_{31} = (1-\Gamma^2)\frac{3\mu^2}{4(9+\mu^2)^2}\bar{b}_2\bar{b}_4$$

$$\tilde{a}_{13} = (1-\Gamma^2)\frac{3\mu^2}{4(1+9\mu^2)^2}\bar{b}_2\bar{b}_3$$

(62)

4.3 Minimization of Total Potential Energy

The total potential energy must be a minimum when the structure is in equilibrium and this condition leads to the following equations

$$\frac{\partial\bar{U}_2}{\partial\bar{b}_2}=0 \qquad \frac{\partial\bar{U}_2}{\partial\bar{b}_3}=0 \qquad \frac{\partial\bar{U}_2}{\partial\bar{b}_4}=0$$

(63)

Substitution of Eq. (61) into Eq. (63) leads to three equilibrium conditions as follows:

$$\bar{\phi}_1\frac{\beta}{1-\Gamma} = \bar{A}_1+\beta^2(\bar{A}_2+\bar{A}_3\eta+\bar{A}_4\eta^2)+\bar{b}_2^2\bar{A}_5 \qquad (64)$$

$$\bar{\phi}_2 \frac{\beta}{1-\Gamma} = \bar{B}_1 + \beta^2 \bar{B}_4 \eta^2 + \bar{b}_2^2 \left(\bar{B}_5 + \frac{\bar{B}_6}{\eta} \right) \tag{65}$$

$$\bar{\phi}_3 \frac{\beta}{1-\Gamma} = \bar{H}_1 + (\bar{H}_2 + \bar{H}_4 \eta^2) \beta^2 + \bar{b}_2^2 (\bar{H}_5 + \frac{\bar{H}_6}{\eta}) \tag{66}$$

where

$$\bar{\phi}_1 = \frac{3}{2} \bar{\sigma} + \bar{\sigma}_b - \mu^2 \frac{3\bar{p}}{2}$$

$$\bar{A}_1 = \frac{(1+\mu^2)^2}{8(1-\nu^2)} + \bar{S}_1$$

$$\bar{A}_2 = \frac{1}{(1+\mu^2)^2}$$

$$\bar{A}_3 = -\left[\frac{(2+\Gamma)(1+\eta_1)}{(1+\mu^2)^2} \cdot \frac{3\mu^2}{2} + \frac{3\mu^2}{8} \eta_1 \right]$$

$$\bar{A}_4 = (1+\Gamma) \left\{ \frac{9(1+\eta_1)^2 \mu^4}{4(1+\mu^2)^2} + \frac{9\mu^4}{4} \left[\frac{\eta_1^2}{(9+\mu^2)^2} + \frac{1}{(1+9\mu^2)^2} \right] \right\}$$

$$\bar{A}_5 = (1+\Gamma) \cdot \frac{9(1+\mu^4)}{256}$$

$$\bar{S}_1 = \sum_{k=1}^{N_k} \frac{\bar{E}_k \bar{I}_k \bar{l}_k}{2} \left[\frac{3}{2} (C_1^4 + 6\mu^2 C_1^2 C_2^2 + \mu^4 C_2^4) \right]$$

$$+ \sum_{j=1}^{N_j} \frac{\bar{E}_j \bar{I}_j \bar{l}_j}{2} \left[\frac{3}{2} (C_3^4 + 6\mu^2 C_3^2 C_4^2 + \mu^4 C_4^4) \right]$$

$$+ \sum_{k=1}^{N_k} \frac{3 \bar{G}_k \bar{J}_k \bar{l}_k}{8} \left[(C_1 + \mu C_2)^2 (C_2 - \mu C_1)^2 + (C_1 - \mu C_2)^2 (C_2 + \mu C_1)^2 \right]$$

$$+ \sum_{j=1}^{N_j} \frac{3 \bar{G}_j \bar{J}_j \bar{l}_j}{8} \left[(C_3 + \mu C_4)^2 (C_4 - \mu C_3)^2 + (C_3 - \mu C_4)^2 (C_4 + \mu C_3)^2 \right]$$

(67)

$$\bar{\phi}_2 = -\mu^2 \frac{3\bar{p}}{2}$$

$$\bar{B}_1 = \frac{\mu^4}{2(1-\nu^2)} + \bar{S}_2$$

$$\bar{B}_4 = (1+\Gamma)\frac{9\mu^4}{8(1+\mu^2)^2}\eta_1^2$$

$$\bar{B}_5 = (1+\Gamma)\left[\frac{9\mu^4}{32(1+\mu^2)^2}(1+\eta_1) + \frac{9\mu^4}{32(1+9\mu^2)^2}\right]$$

$$\bar{B}_6 = -\frac{3\mu^2}{16(1+\mu^2)^2}$$

$$\bar{S}_2 = \sum_{k=1}^{N_k} 3\bar{E}_k\bar{I}_k\bar{l}_k\mu^4 C_2^4 + \sum_{j=1}^{N_j} 3\bar{E}_j\bar{I}_j\bar{l}_j\mu^4 C_4^4$$
$$+ \sum_{k=1}^{N_k} 3\bar{G}_k\bar{J}_k\bar{l}_k\mu^4 C_1^2 C_2^2 + \sum_{j=1}^{N_j} 3\bar{G}_j\bar{J}_j\bar{l}_j\mu^4 C_3^2 C_4^2$$

(68)

$$\bar{\phi}_3 = \bar{\sigma}_b + \frac{3}{2}\bar{\sigma}$$

$$\bar{H}_1 = \frac{1}{2(1-\nu^2)} + \bar{S}_3$$

$$\bar{H}_2 = \frac{1}{4}$$

$$\bar{H}_4 = (1+\Gamma)\frac{36\mu^4}{32(1+\mu^2)^2}$$

$$\bar{H}_5 = (1+\Gamma)\left[\left(1+\frac{1}{\eta_1}\right)\frac{1}{(1+\mu^2)^2} + \frac{1}{(9+\mu^2)^2}\right]\cdot\frac{9\mu^4}{32}$$

$$\bar{H}_6 = -(1+\Gamma)\frac{3\mu^2}{128\eta_1} - \frac{3\mu^2}{16(1+\mu^2)^2\eta_1}$$

$$\bar{S}_3 = \sum_{k=1}^{N_k} 3\bar{E}_k\bar{I}_k\bar{l}_k\, C_1^4 + \sum_{j=1}^{N_j} 3\bar{E}_j\bar{I}_j\bar{l}_j\, C_3^4 + \sum_{k=1}^{N_k} 3\bar{G}_k\bar{J}_k\bar{l}_k\, C_2^2 C_1^2 + \sum_{j=1}^{N_j} 3\bar{E}_j\bar{I}_j\bar{l}_j\, C_3^2 C_4^2 \tag{69}$$

Eliminating β and $\bar{b}_2$ from Eqs. (64), (65) and (66), the following equation is obtained:

$$\bar{M}_1 \bar{\Phi}_2^2 + \bar{M}_2 \bar{\Phi}_2 + \bar{M}_3 = 0 \tag{70}$$

where

$$\bar{M}_1 = \frac{1}{(1-\Gamma^2)}\left[\frac{\bar{D}_2\bar{D}_3}{\bar{F}_3^2}\left(\bar{H}_5 + \frac{\bar{H}_6}{\eta} - \bar{A}_5\right)^2 + \frac{\bar{F}_2}{\bar{F}_3}\left(\bar{B}_5 + \frac{\bar{B}_6}{\eta}\right)^2 - \left(\frac{\bar{F}_2\bar{D}_3}{\bar{F}_3^2} + \frac{\bar{D}_2}{\bar{F}_3}\right)\left(\bar{H}_5 + \frac{\bar{H}_6}{\eta} - \bar{A}_5\right)\left(\bar{B}_5 + \frac{\bar{B}_6}{\eta}\right)\right]$$

$$\bar{M}_2 = -\frac{\mu^2\bar{P}}{(1-\Gamma^2)}\left\{\frac{2\bar{D}_2\bar{D}_3}{\bar{F}_3^2}\left(\bar{H}_5 + \frac{\bar{H}_6}{\eta}\right)\left(\bar{H}_5 + \frac{\bar{H}_6}{\eta} - \bar{A}_5\right) + \frac{2\bar{F}_2}{\bar{F}_3}\left(\bar{B}_5 + \frac{\bar{B}_6}{\eta} - \bar{A}_5\right) - \left(\frac{\bar{F}_2\bar{D}_3}{\bar{F}_3^2} + \frac{\bar{D}_2}{\bar{F}_3}\right)\left[\bar{A}_5^2 + 2\left(\bar{B}_5 + \frac{\bar{B}_6}{\eta}\right)\left(\bar{H}_5 + \frac{\bar{H}_6}{\eta}\right) - \bar{A}_5\left(\bar{B}_5 + \frac{\bar{B}_6}{\eta} + \bar{H}_5 + \frac{\bar{H}_6}{\eta}\right)\right]\right\}$$

$$\bar{M}_3 = \frac{\mu^4 \bar{P}^2}{(1-\Gamma^2)}\Big[\frac{\bar{D}_2\bar{D}_3}{\bar{F}_3^2}\Big(\bar{H}_5+\frac{\bar{H}_6}{\eta}\Big)^2+\frac{\bar{F}_2}{\bar{F}_3}\Big(\bar{B}_5+\frac{\bar{B}_6}{\eta}-\bar{A}_5\Big)^2$$
$$-\Big(\frac{\bar{F}_2\bar{D}_3}{\bar{F}_3^2}+\frac{\bar{D}_2}{\bar{F}_3}\Big)\Big(\bar{H}_5+\frac{\bar{H}_6}{\eta}\Big)\Big(\bar{B}_5+\frac{\bar{B}_6}{\eta}-\bar{A}_5\Big)\Big]$$
$$+\frac{\bar{F}_2^2\bar{D}_3^2}{\bar{F}_3^2}-2\frac{\bar{D}_2\bar{D}_3\bar{F}_2}{\bar{F}_3}+\bar{D}_2^2$$

(71)

$$\bar{D}_2 = \bar{A}_1\Big(\bar{B}_5+\frac{\bar{B}_6}{\eta}\Big)-\bar{B}_1\bar{A}_5$$
$$\bar{D}_3 = (\bar{A}_2+\bar{A}_3\eta+\bar{A}_4\eta^2)\Big(\bar{B}_5+\frac{\bar{B}_6}{\eta}\Big)-\bar{B}_4\bar{A}_5\eta^2$$
$$\bar{F}_2 = \bar{A}_1\Big(\bar{H}_5+\frac{\bar{H}_6}{\eta}\Big)-\bar{H}_1\bar{A}_5$$
$$\bar{F}_3 = (\bar{A}_2+\bar{A}_3\eta+\bar{A}_4\eta^2)\Big(\bar{H}_5+\frac{\bar{H}_6}{\eta}\Big)-(\bar{H}_2+\bar{H}_4\eta^2)\bar{A}_5$$

(72)

and

$$\bar{\Phi}_2 = \bar{\sigma}_b + \frac{3}{2}\bar{\sigma} \qquad (73)$$

Eq. (70) is the equation for the stationary load of a stiffened shell under bending load. Numerical calculations of the minimum stress parameter $\bar{\Phi}_2$ are given in Chapter VI.

CHAPTER V

INSTABILITY OF A STIFFENED CYLINDRICAL SHELL UNDER TRANSVERSE LOAD AND INTERNAL PRESSURE

5.1 Deflection Pattern and Approximate Stress Function

When a long cylindrical shell is subjected to transverse shear load at one end, an approximate form of the deflection pattern can be assumed as in the bending case in the previous chapter in Eq. (53). The deflection shape is

$$w = b_1 + \cos^2\left(\frac{y}{2R}\right)\left(b_2 \cos\frac{mx}{R}\cos\frac{ny}{R} + b_3\cos\frac{2mx}{R} + b_4\cos\frac{2ny}{R}\right) \tag{53}$$

Corresponding to this deflection pattern, the stress function F is proposed

$$\begin{aligned} F = &-\frac{P}{\pi t}\, x\cos\frac{y}{R} + \frac{pR}{t}\,\frac{x^2}{2} + a_{11}\cos\frac{mx}{R}\cos\frac{ny}{R} \\ &+ a_{22}\cos\frac{2mx}{R}\cos\frac{2ny}{R} + a_{20}\cos\frac{2mx}{R} + a_{02}\cos\frac{2ny}{R} \\ &+ a_{31}\cos\frac{3mx}{R}\cos\frac{ny}{R} + a_{13}\cos\frac{mx}{R}\cos\frac{3ny}{R} \end{aligned} \tag{74}$$

The relations between the coefficients a_{11}, a_{22}, a_{02}, a_{20}, a_{13}, a_{31}, and b_2, b_3, b_4 are given in Eq. (57), and $\bar{b}_1$ is the same as given in Eq. (58).

5.2 Expressions of Total Potential Energy

The total potential energy of this system is the sum of the strain energy and the potential of the applied loads.

$$U_3 = U_e + U_b + U_p + U_s + U_f + U_{b,k} + U_{b,j} + U_{T,k} + U_{T,j} \qquad (75)$$

If w, F, and $\bar{b}_1$ as given by Eqs. (53), (58), and (74), respectively, are substituted in Eq. (75), and the integration carried out, the total potential is obtained in the following form:

$$\begin{aligned}\bar{U}_3 = \frac{U_3 R}{E\pi t^3 L} = &-\bar{P}^2 + \bar{p}^2 - 2(1+\nu)\bar{P}^2 + (1+\nu)\left(\frac{R}{\ell}\right)^2 \bar{P}^2 \\ &-(1-\Gamma^2)\left(\frac{\bar{b}_2^2}{8} + \bar{b}_4^2\right)\frac{\bar{P}}{4\beta} + \frac{\bar{P}^2}{6} + 2\bar{p}\left\{\frac{(1-\Gamma^2)}{4\beta}\left[\frac{\bar{b}_2^2}{8}\mu^2\right.\right. \\ &\left.\left. + \frac{\bar{b}_2^2}{16}\left(\mu^2 + \frac{1}{m^2}\right) + \bar{b}_3^2\mu^2 + \frac{\bar{b}_3^2}{4}\left(2\mu^2 + \frac{1}{2m^2}\right) + \frac{\bar{b}_4^2}{8m^2}\right] - \bar{p}\right\} \\ &+ \bar{a}_{11}^2 \frac{(1+\mu^2)^2}{4\beta^2} + \bar{a}_{22}^2 \frac{4(1+\mu^2)^2}{\beta^2} + \bar{a}_{20}^2 \frac{8}{\beta^2} + \bar{a}_{02}^2 \frac{8\mu^4}{\beta^2} +\end{aligned}$$

$$+\bar{a}_{31}^2\frac{(9+\mu^2)^2}{4\beta^2}+\bar{a}_{13}^2\frac{(1+9\mu^2)^2}{4\beta^2}+\frac{(1-\Gamma)^2}{192\beta^2(1-\nu^2)}\left\{\bar{b}_2^2(1+\mu^2)^2\right.$$
$$+\frac{\bar{b}_2^2}{2}\left[(1+\mu^2)^2+\frac{6\mu^2}{m^2}+\frac{2}{m^2}+\frac{1}{m^4}\right]+\bar{b}_4^2\left(48+\frac{8}{m^2}+\frac{1}{m^4}\right)$$
$$\left.+\bar{b}_3^2\left(48\mu^4+24\frac{\mu^2}{m^2}+\frac{1}{m^4}\right)\right\}+\bar{U}_{b,k}+\bar{U}_{b,j}+\bar{U}_{T,k}+\bar{U}_{T,j} \tag{76}$$

where $\bar{U}_{b,k}$, $\bar{U}_{b,j}$, $\bar{U}_{T,k}$, $\bar{U}_{T,j}$ are the same as those obtained in the bending case Eq. (60).

where β, μ and Γ are given in Eqs. (22) and (6), and

$$\bar{P}=\frac{PL}{E\pi Rt^2} \tag{77}$$

For the same reason as mentioned in the previous chapter, $1/m^2$ and $1/m^4$ can be neglected compared to unity in Eq. (76). The total potential energy is finally obtained in the following form:

$$\bar{\bar{U}}_3=-\frac{5}{6}\bar{P}^2+\bar{P}^2-2(1+\nu)\bar{P}^2+(1+\nu)\left(\frac{R}{l}\right)^2\bar{P}^2$$
$$-(1-\Gamma^2)\left(\frac{\bar{b}_2^2}{8}+\bar{b}_4^2\right)\cdot\frac{\bar{P}}{4\beta}+2\bar{P}\left[\frac{(1-\Gamma^2)}{4\beta}\left(\frac{\bar{b}_2^2}{8}+\bar{b}_3^2\right)\cdot\frac{3\mu^2}{2}\right.$$
$$\left.-\bar{P}\right]+\tilde{a}_{11}^2\frac{(1+\mu^2)^2}{4\beta^2}+\tilde{a}_{22}^2\frac{4(1+\mu^2)^2}{\beta^2}+\tilde{a}_{20}^2\left(\frac{8}{\beta^2}\right)+\tilde{a}_{02}^2\left(\frac{8\mu^4}{\beta^2}\right)$$
$$+\tilde{a}_{13}^2\frac{(9+\mu^2)^2}{4\beta^2}+\tilde{a}_{31}^2\frac{(1+9\mu^2)^2}{4\beta^2}+$$

$$+\frac{(1-\Gamma)^2}{192\,\beta^2(1-\nu^2)}\left[\bar{b}_2^2(1+\mu^2)^2\frac{3}{2}+\bar{b}_3^2\mu^4\cdot 48+\bar{b}_4^2\cdot 48\right] \qquad (78)$$
$$+U_{b,k}+U_{b,j}+U_{\tau,k}+U_{\tau,j}$$

where $\tilde{a}_{11}$, $\tilde{a}_{22}$, $\tilde{a}_{02}$, $\tilde{a}_{20}$, $\tilde{a}_{31}$, and $\tilde{a}_{13}$ are given in Eq. (62).

5.3 Minimization of Total Potential Energy

By variation of the total potential energy in Eq. (78) with respect to each of the arbitrary parameters, three simultaneous equations are obtained. From these three equations, two arbitrary parameters ($\bar{b}_2$ and β) can be eliminated. Finally, a governing equation for the stationary load of a stiffened shell under transverse shear load is obtained:

$$\bar{M}_1\bar{\Phi}_3^2+\bar{M}_2\bar{\Phi}_3+\bar{M}_3=0 \qquad (79)$$

where

$$\bar{\Phi}_3=\frac{\bar{P}}{2} \qquad (80)$$

$\bar{M}_1$, $\bar{M}_2$, and $\bar{M}_3$ are given in Eq. (71).

CHAPTER VI

NUMERICAL EXAMPLES

The minimum stresses are to be found from Eqs. (49), (70), or (79) for the various types of loading. In each case, the stress parameters ($\bar{\sigma}_c$, Φ_2 and Φ_3) are functions of three free parameters η, η_1, and μ. While μ is the wave-length ratio, the expression η and η_1, can be considered as deflection parameters ratio. The minimum values are found numerically at various inclined angles, stiffeners rigidity and the internal pressure. Numerical calculations were made on the IBM 709. Program I is for finding minimum stress $\bar{\sigma}_c$ for axial compression case. Program II is for finding minimum stress parameters, Φ_2 and Φ_3. The minimum stress can be found with any given numerical data. In the following, some examples are given.

6.1 Cylinder under Bending and Internal Pressure or Transverse Load and Internal Pressure

In this part of calculation, the cylinder is assumed perfect, i.e., $\Gamma = 0$ [Eq. (6)], and the angles of the inclined stiffeners with the generator are equal, i.e.,

$\gamma_1 = \gamma_2 = \gamma$. Poisson's ratio is 1/3. The general characteristics are assumed:

$$\bar{I}_k = \bar{I}_j \quad , \quad \bar{J}_k = \bar{J}_j \quad , \quad \bar{G}_k = \bar{G}_j \quad , \quad \bar{l}_k = \bar{l}_j$$

$$\sum_{k=1}^{N_k} \bar{E}_k \bar{I}_k \bar{l}_k = \sum_{j=1}^{N_j} \bar{E}_j \bar{I}_j \bar{l}_j = \frac{\bar{E}\,\bar{I}\,\bar{l}}{2} \quad , \quad N_k = N_j$$

$$K = \frac{\sum_{j=1}^{N_j} \bar{G}_j \bar{J}_j}{\sum_{j=1}^{N_j} \bar{E}_j \bar{I}_j} = \frac{\sum_{k=1}^{N_k} \bar{G}_k \bar{J}_k}{\sum_{k=1}^{N_k} \bar{E}_k \bar{I}_k} \tag{81}$$

By substituting Eq. (81) into Eq. (70), the value of Φ_2 as a function of η, η_1 and μ is found. First, Φ_2 versus η is plotted for various values of μ at a fixed value of η_1, in Figs. 4, 5, 6, 7, 8, and 9. Minimum Φ_2 found from each of these curves is called $\Phi_{2,\eta}$. It should be equivalent to the value found from the relation $\partial \Phi_2 / \partial \eta = 0$. Then $\Phi_{2,\eta}$ versus μ is plotted for various η_1 in Fig. 10. Minimum $\Phi_{2,\eta}$ found from each of these curves is called $\Phi_{2,\eta,\mu}$, plotted in Fig. 11. It should be equivalent to the value found from the relation $\partial \Phi_{2,\eta} / \partial \mu = 0$. This minimum value is the dimensionless critical stress $(\bar{\sigma}_b + 3/2\, \bar{\sigma})_{cr}$ for the shell with inclined stiffeners at an angle of $\gamma = 45^{\circ}$ with the generator. By the same procedure as in the previous case,

the curves of $\Phi_{2,\eta,\mu}$ versus η_1 for various inclined stiffeners at an angle of $\gamma = 0^\circ$ (stringers), 30°, 60°, and 90° (rings) are found and shown in Fig. 12. The minimum value of each of these curves is plotted in Fig. 13. The relation between minimum stress parameter $\Phi_{2,\eta,\mu}$ and stiffeners rigidity, $\bar{E}\,\bar{I}\,\bar{\ell}$, is shown in Fig. 14. The relation between minimum stress parameter $\Phi_{2,\eta,\mu}$ and internal pressure $\bar{p}$ is also plotted in Fig. 15.

If Φ_3 is replaced by Φ_2 in Eq. (79), the equation is the same as the one obtained in the bending case. Therefore, the minimum stress for the case of transverse shear can be found by using $\Phi_{3,\eta,\mu}$ instead of $\Phi_{2,\eta,\mu}$ in all the figures from Fig. 4 to Fig. 15. Where

$$\Phi_{3,\eta,\mu} = \left(\frac{\bar{P}}{2}\right)_{cr.}$$

$$\Phi_{2,\eta,\mu} = \left(\bar{\sigma}_b + \frac{3}{2}\bar{\sigma}\right)_{cr.}$$

6.2 Cylinder under Axial Compression and Internal Pressure

By the same procedure as in the previous section we can find the minimum stress, $\bar{\sigma}_c$ from Eq. (49) by Program I in Appendix B. In this part of calculation, a numerical

example is given for comparison of the effect of the imperfection in shells at various inclined angles. This is plotted in Fig. 16.

CHAPTER VII

EXPERIMENTAL INVESTIGATION

A group of tests for the general instability of rings and/or stringers stiffened shells have been made by many authors, but up to the present time, no work has been done on the experimental investigation of the general instability of inclined stiffened cylinders subject to axial compression or bending. Therefore, it was necessary to conduct a series of tests in order to compare experimental with the theoretical results.

7.1 Models

The models used in these series of tests were stiffened cylindrical shells constructed from Du Pont Mylar of 1000 gage (0.01 inches), type A. Tests indicated that the Mylar sheet has a Young's modulus E varied from 550,000 psi to 780,000 psi and Poisson's ratio of 1/3. In the numerical calculation to follow, the value of E is taken to be 700,000 psi.

All of the models were made by rolling the Mylar sheet around a thick-walled steel tube and joining the

ends with a 3/4 inch wide strip of double-faced Scotch tape. It appears that these joints might stiffen that part of the cylinder appreciably. However, reports from various investigators indicate that this is not the case, since buckling waves appear across the joint with no noticeable change in pattern. The present tests have confirmed this observation. The inside radius of the cylinders was 4 inches, while the length was 9 inches. The stiffeners were made by cutting the Mylar tape to a band-width of 3/8 inch. The thickness of each layer of the tape was 0.01 inch. All the specimens had stiffeners made of two layers of the Mylar tape (i.e., nominal thickness of the stiffeners = 0.02 inch). The double-faced Scotch tape was used to join the layers of Mylar tape. It was also used to bond the stiffeners with the cylindrical shells. The adhensive tape was not effective when more than two layers of Mylar tape were used as stiffeners. The spacing between two neighboring stiffeners was 1 1/4 inches. The stiffeners were inclined at angles of $\gamma = 30^{\circ}$, 45°, and 60° with the generator of the cylinders. In order to provide additional information for the numerical example of the previous chapter, the dimensions of the stiffened shells used in the experiments were the same as those considered in that example.

7.2 Test Result

The cylinders were mounted vertically on the test machine. The upper adaptor has two pivot pins fixed diametrically at its edge. The pins are supported by horizontal bearings which are fixed to the frame of the test stand. When a moment is applied to make the upper adaptor rotate about its pivot pins, this transmits the bending moment to the cylinder. The lower adaptor is connected to a circular plate which can be moved up and down so that the axial loading can be transmitted to the cylinder. Bending load is applied by means of a lead screw which pulls a cable up through a bearing which is fixed on the frame of the machine.

The bending moment and the axial compressive loading were found after calibrating the readings from a strain gage indicator. The test results of the stiffened shells subject to axial compression or bending without internal pressure at an angle of $\gamma = 30^{\circ}$, 45°, or 60° are tabulated in Table I. Some of the results are plotted in Fig. 18. The deformed pattern after buckling at $\bar{p} = 0$ are shown in Fig. 17. The buckle pattern formed across the seam with no distortion in shape and none of the seams failed during buckling.

CHAPTER VIII

DISCUSSIONS AND CONCLUSIONS

In the previous chapters, nonlinear analysis on cylinders with inclined stiffeners have been made by the energy method. From the numerical examples the following observations are made:

1. From Fig. 13, it can be observed that the minimum stress parameter $\Phi_{2,\eta,\mu}$ increases with increasing stiffeners' rigidity, and the optimum inclined angle varies with the rigidity. In the present example, it has been found that the most effective inclined angle is in the neighborhood of $\gamma = 60^{\circ}$.

2. In Fig. 14, strength of cylinder with stiffener inclined at $\gamma = 45^{\circ}$ is compared with that of ring-stiffened cylinder. At smaller stiffeners' rigidity, the ring-stiffened cylinder is stronger, but at higher rigidity, the inclined stiffened cylinders have more strength. The minimum stress of ring-stiffened shells approaches to the buckling stress found from small-deflection

solutions as a limit, while the inclined stiffened cylinder continues to increase with increasing rigidity ($\bar{E}\ \bar{I}\ \bar{\ell}$). In the same figure, the consideration of torsional rigidity (for example K = 1/2) is compared with the result including the bending rigidity only (i.e., K = 0). The difference between these results increases with rigidity, $\bar{E}\ \bar{I}\ \bar{\ell}$. However, the general relation of the minimum stress with other parameters will remain the same.

3. Example of the variation of $\Phi_{2,\eta,\mu}$ versus $\bar{p}$ is shown in Fig. 15. For other combinations of γ, K and $\bar{E}\ \bar{I}\ \bar{\ell}$, the curve will be similar but different numerically.

4. The minimum stress of cylinder under axial compression versus the various inclined angles is shown in Fig. 16. Imperfect cylinder (Γ = 0.3) has lower strength as expected. The evaluating of Γ can be referred to Ref. (22). The effect of imperfection for stiffened cylinders is smaller in comparison with the unstiffened cylinder.

5. The buckling patterns of the unpressurized-stiffened shells subject to axial compression are shown in Fig. 17. The deformed pattern after buckling is diamond-shaped and across the inclined stiffeners as expected.

6. In Fig. 18, it can be observed that the theory for the bending case is in reasonable agreement with tests on the Mylar inclined-stiffened cylindrical shells.

This study has presented the approximate solutions by energy method. Nevertheless, the results of this analysis should give some insight into the problems of the general instability of stiffened shells with inclined stiffeners.

TABLE I

TESTS OF STIFFENED THIN MYLAR CYLINDERS UNDER AXIAL COMPRESSION OR BENDING WITHOUT INTERNAL PRESSURE

Cylinder Radius = 4 inches
Mylar Nominal Thickness of Shell, t = 0.0075 inches
Thickness of Stiffeners, t_1 = 0.02 inches

Inclined angles	Dimensionless rigidity of stiffeners $\frac{\bar{E}\,\bar{I}}{\bar{\ell}}$	Dimensionless axial compression $\bar{\sigma}_c$	Dimensionless bending stress $\bar{\sigma}_b$
45°	0.059	0.267	0.306
		0.274	0.317
	0.117	0.282	0.312
		0.294	0.329
		0.308	0.317
		0.302	0.306
	0.47	0.287	0.321
		0.339	0.382
		0.322	0.323
	0.94	0.368	0.435
		0.328	0.388
		0.335	0.412
		0.336	0.376
	1.47	0.333	0.365
		0.335	0.365
		0.339	0.358
30°	0.124	0.281	0.306
		0.315	0.321
	0.992	0.302	0.353
		0.322	0.335
		0.314	0.353
60°	0.134	0.288	0.388
		0.322	0.322
	1.072	0.302	0.353
		0.322	0.370
		0.322	0.370

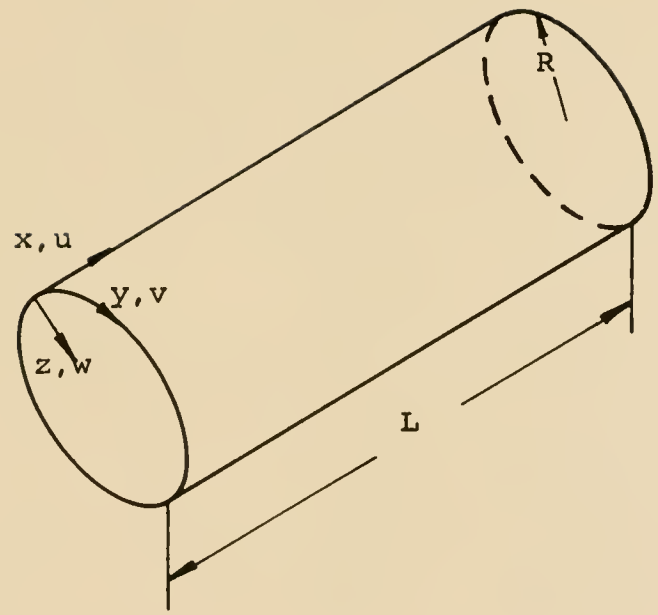

Fig. 1. Coordinates and Displacement Components of a Point on the Middle-Surface of the Shell.

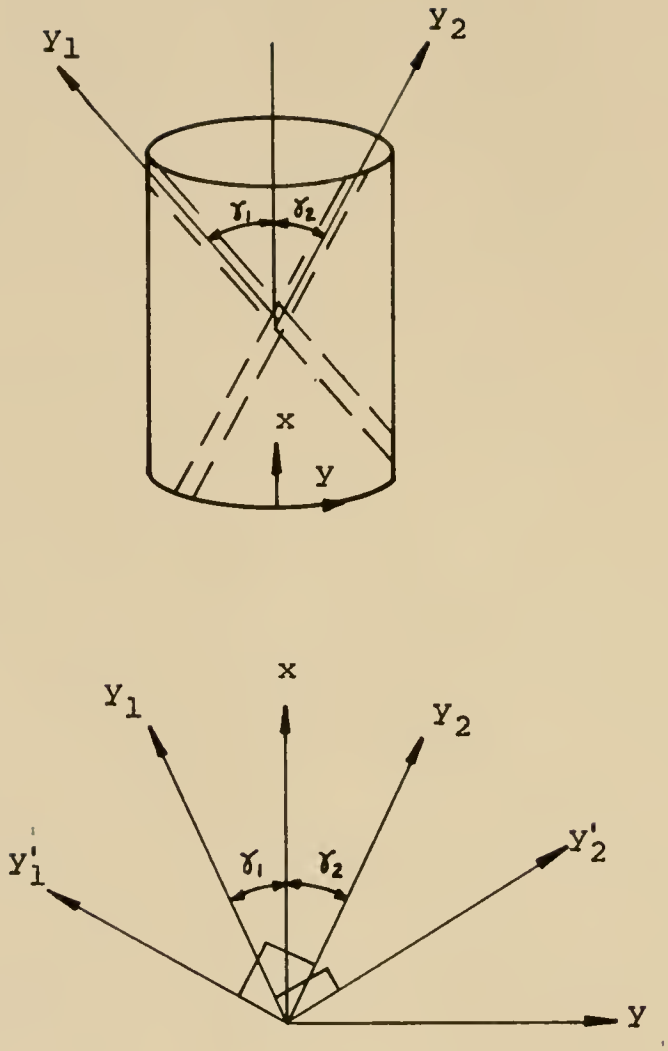

Fig. 2. The Coordinate System of the Stiffened Shells and Stiffeners.

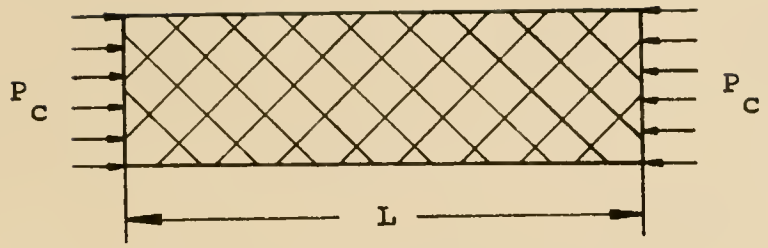

(a) Under Axial Compression P_c

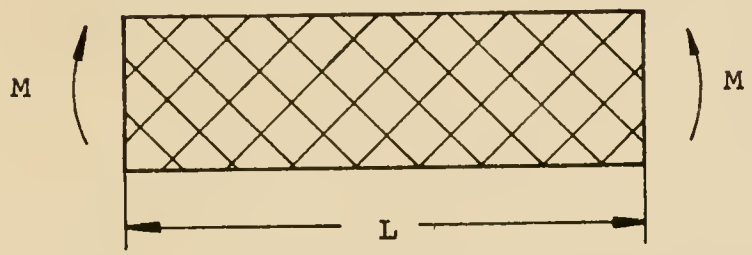

(b) Under Pure Bending M

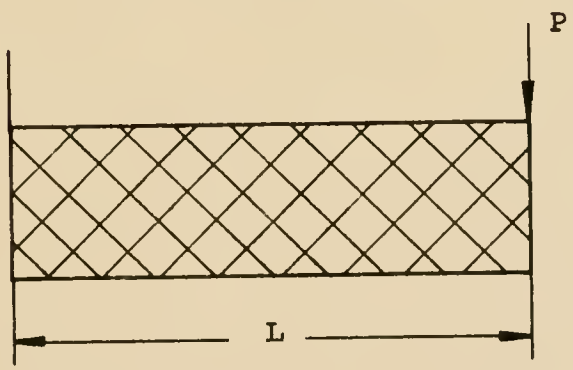

(c) Under Transverse Shear Load P

Fig. 3. The Dimensions of the Stiffened Shells under Different Loadings.

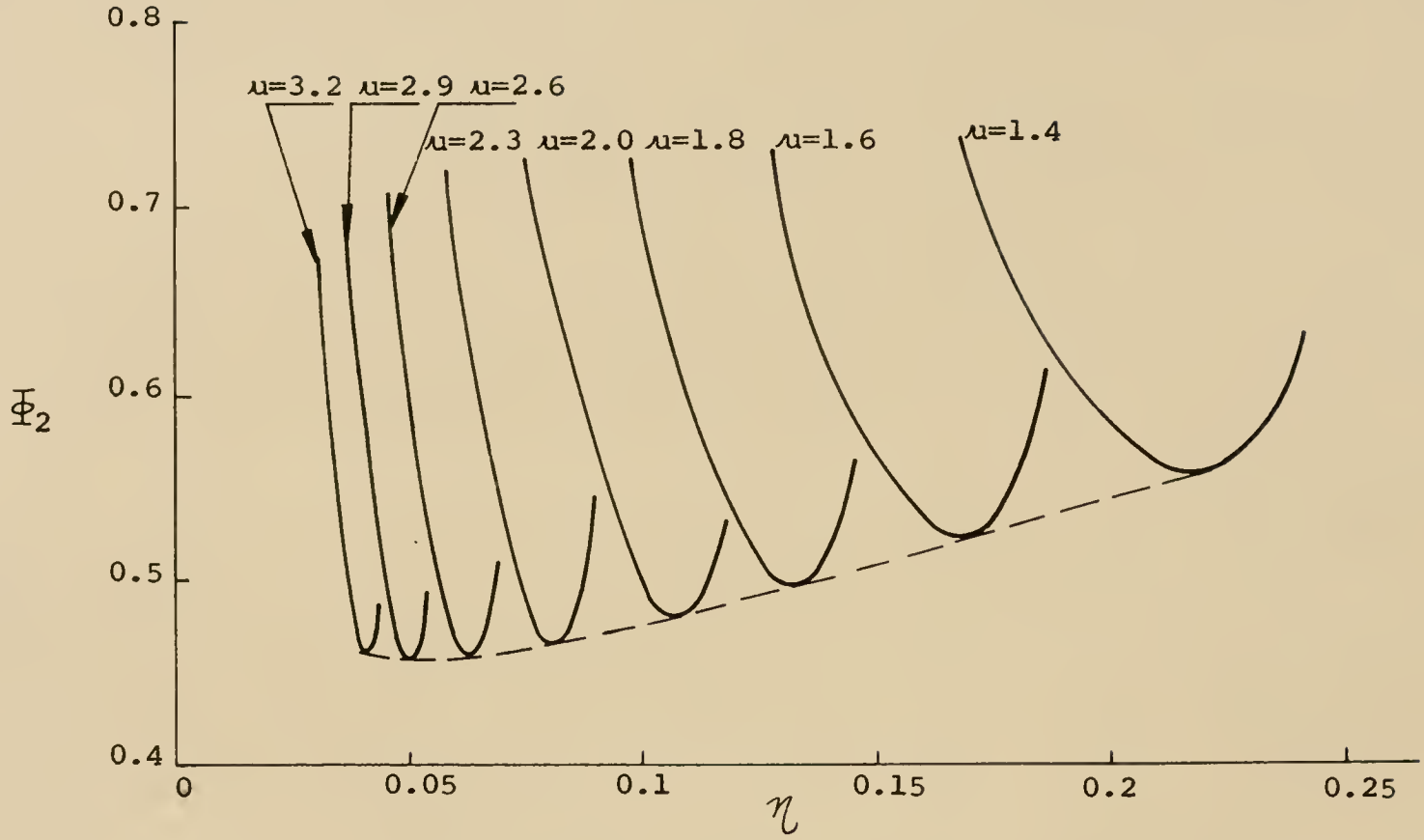

Fig. 4. Stress Parameter Φ_2 as a Function of Deflection η.

($\eta_1 = 0.2$, $\gamma = 45^\circ$, $\bar{E}\,\bar{I}\,\bar{\ell} = 2$, $K = 0$, $\Gamma = 0$, $\bar{p} = 0$)

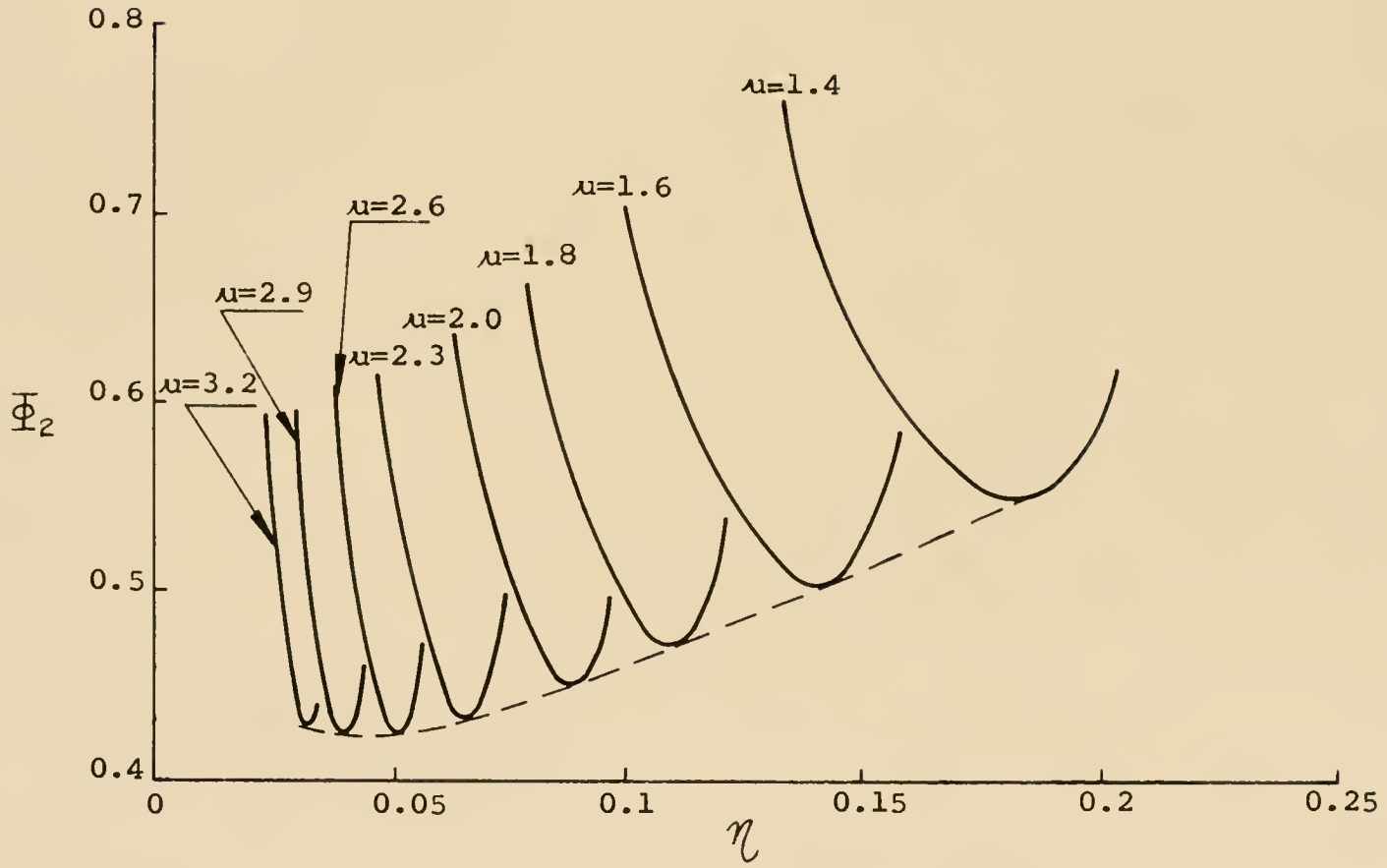

Fig. 5. Stress Parameter Φ_2 as a Function of Deflection η.

($\eta_1 = 0.4$, $\gamma = 45^\circ$, $\bar{E}\,\bar{I}\,\bar{\ell} = 2$, $K = 0$, $\Gamma = 0$, $\bar{p} = 0$)

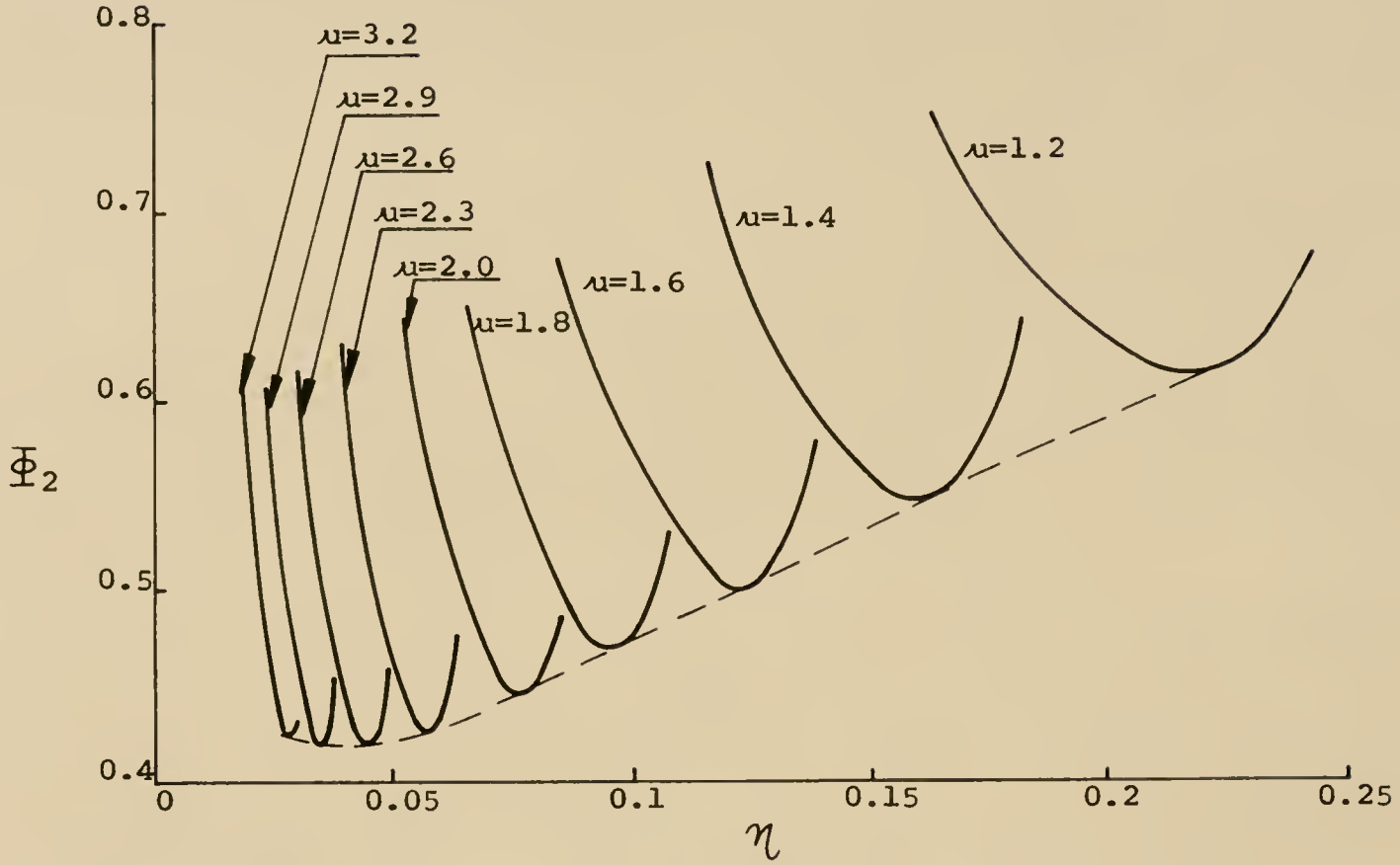

Fig. 6. Stress Parameter Φ_2 as a Function of Deflection η.

($\eta_1 = 0.6$, $\gamma = 45^\circ$, $\bar{E}\,\bar{I}\,\bar{\ell} = 2$, $K = 0$, $\Gamma = 0$, $\bar{p} = 0$)

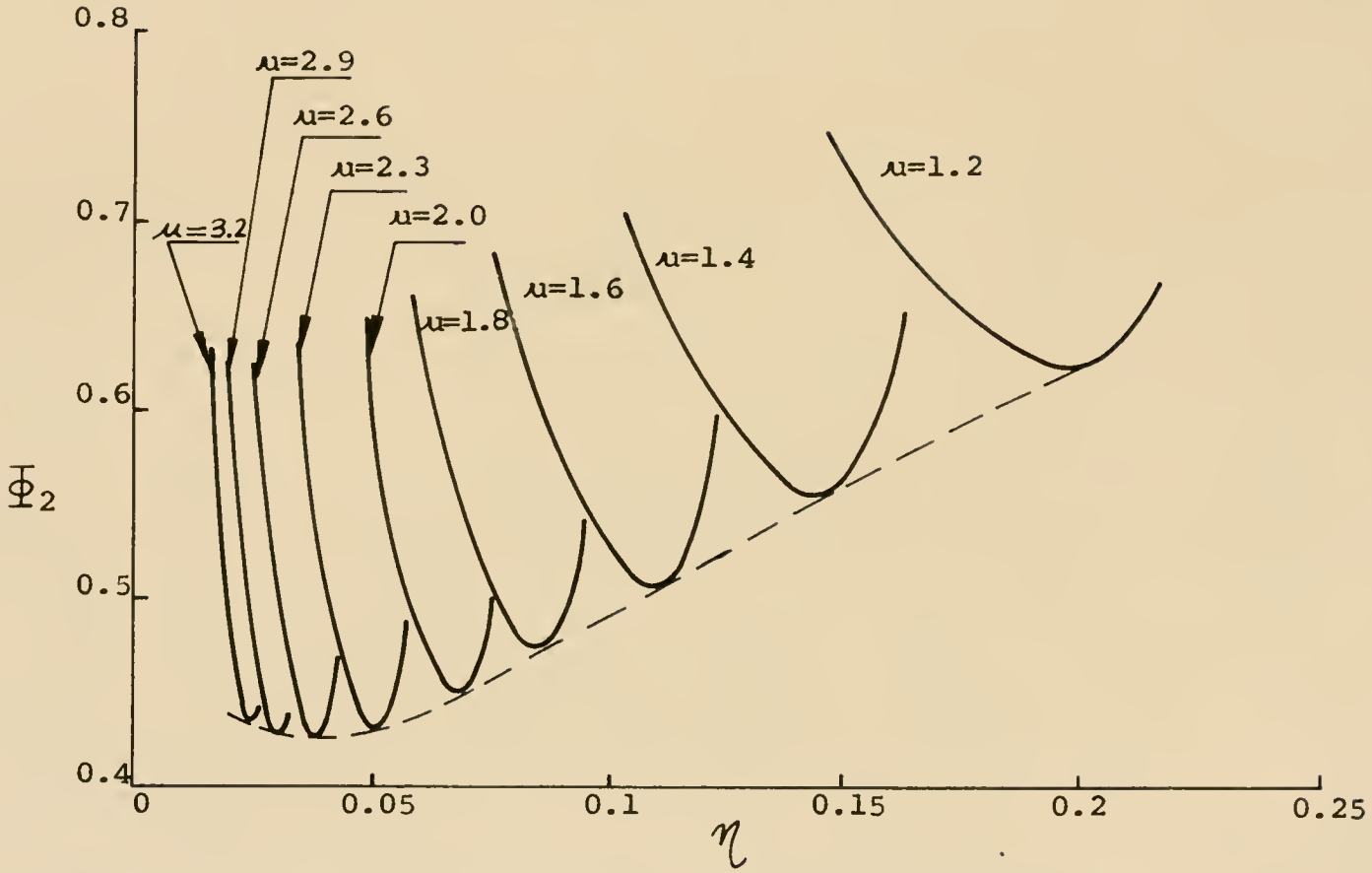

Fig. 7. Stress Parameter Φ_2 as a Function of Deflection η.

(η_1 = 0.8 , γ= 45°, $\bar{E}\,\bar{I}\,\bar{\ell}$ = 2 , K = 0 , Γ= 0 , $\bar{p}$ = 0)

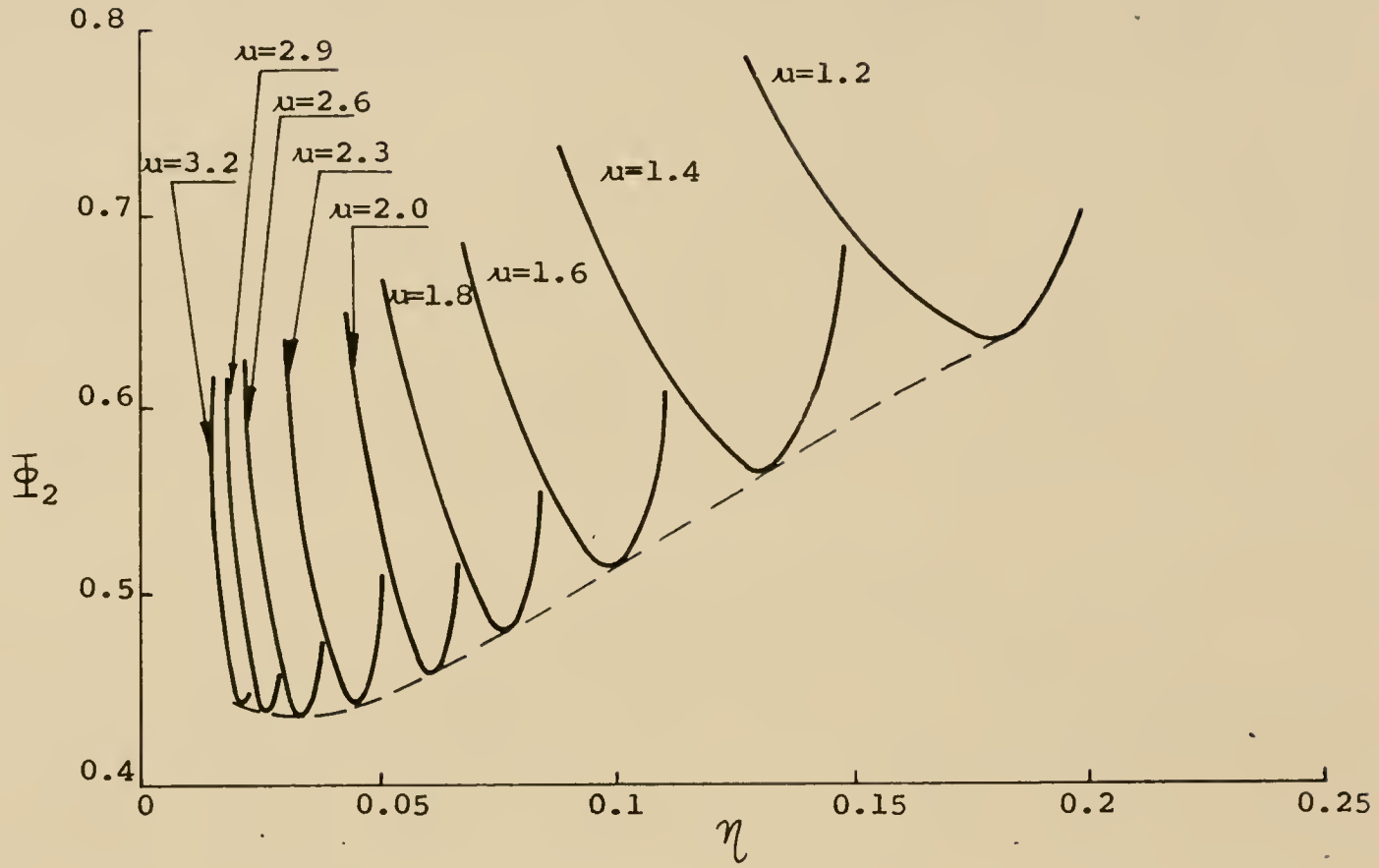

Fig. 8. Stress Parameter Φ_2 as a Function of Deflection η.

($\eta_1 = 1$, $\gamma = 45^\circ$, $\bar{E}\,\bar{I}\,\bar{\ell} = 2$, $K = 0$, $\Gamma = 0$, $\bar{p} = 0$)

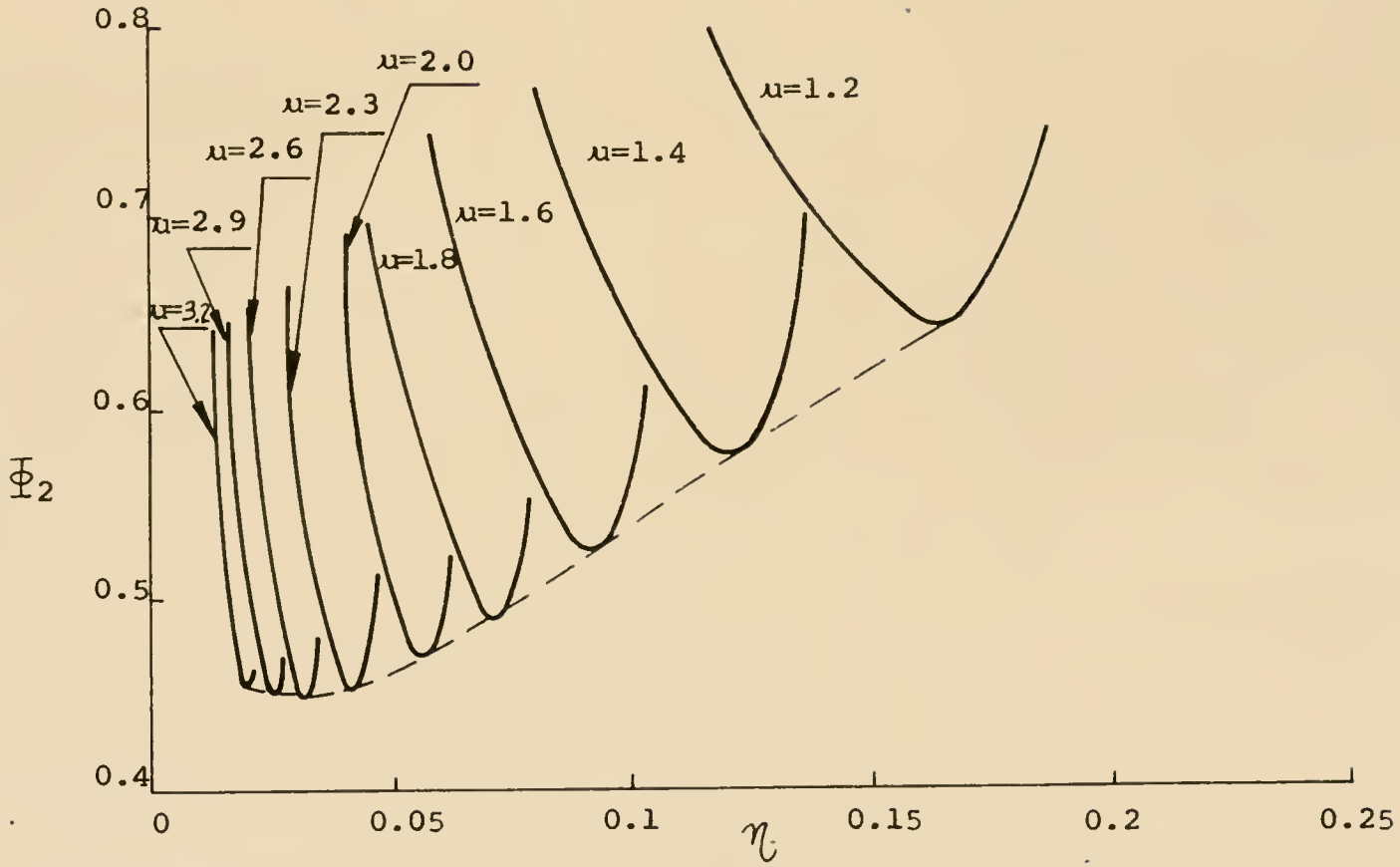

Fig. 9. Stress Parameter Φ_2 as a Function of Deflection η.

($\eta_1 = 1.2$, $\gamma = 45^\circ$, $\bar{E}\,\bar{I}\,\bar{\ell} = 2$, $K = 0$, $\Gamma = 0$, $\bar{p} = 0$)

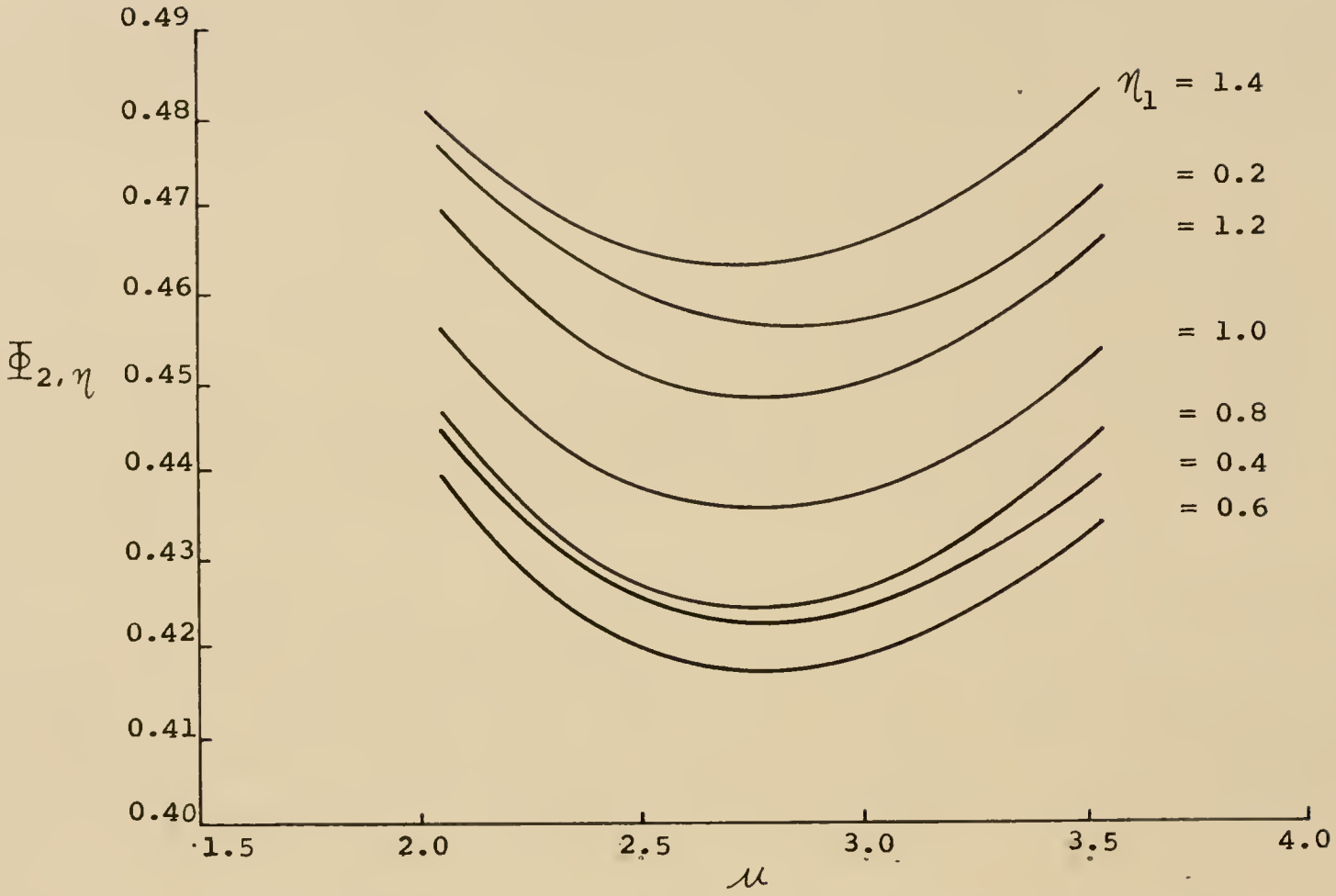

Fig. 10. Stress Parameter $\Phi_{2,\eta}$ as a Function of Wave-Length Ratio μ.

($\gamma = 45^{\circ}$, $\bar{E}\,\bar{I}\,\bar{\ell} = 2$, $K = 0$, $\Gamma = 0$, $\bar{p} = 0$)

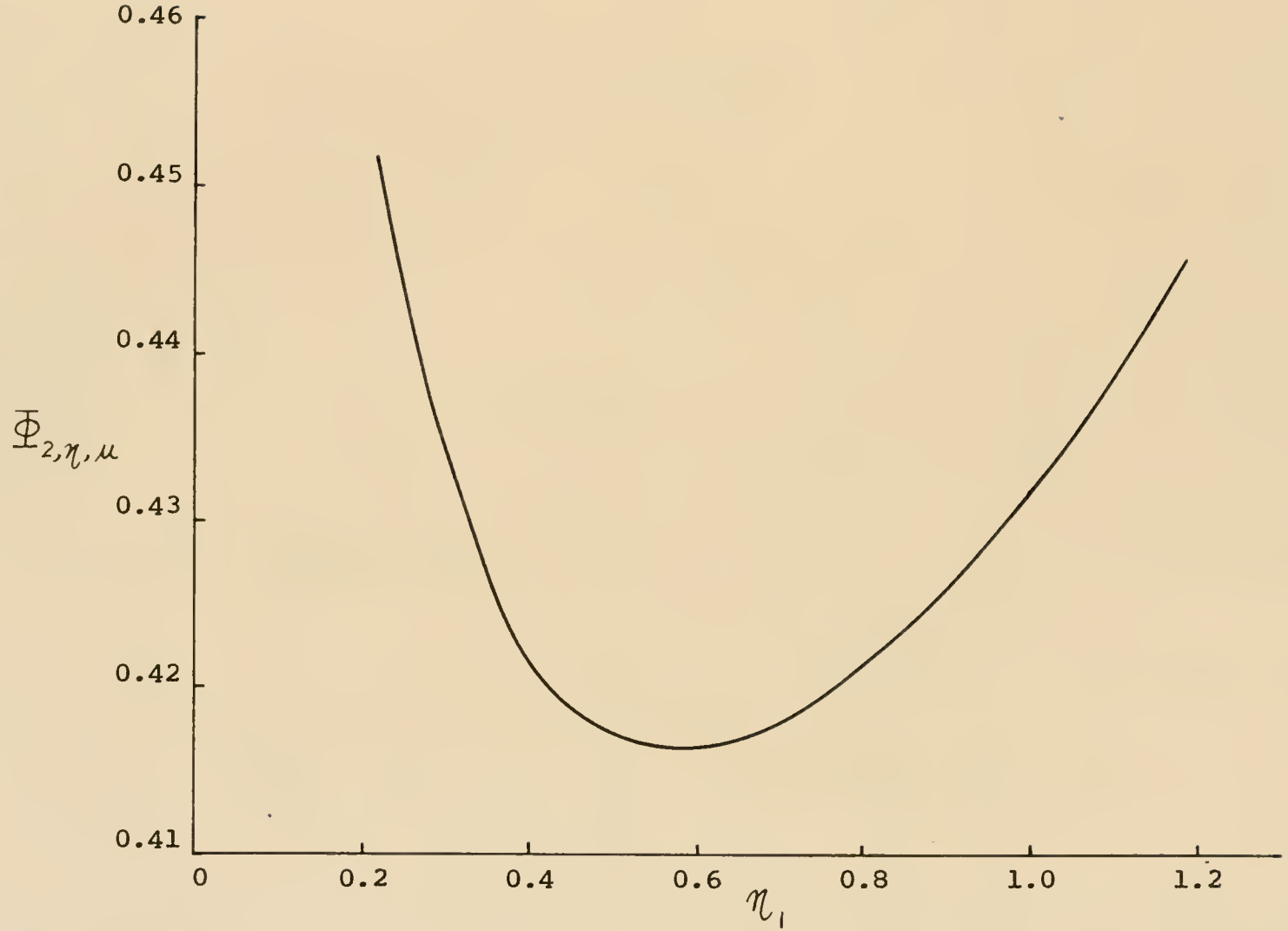

Fig. 11. Minimum Stress Parameter $\Phi_{2,\eta,\mu}$ as a Function of Deflection η_1
($\gamma = 45^{\circ}$, $\bar{E}\,\bar{I}\,\bar{\ell} = 2$, $K = 0$, $\Gamma = 0$, $\bar{p} = 0$)

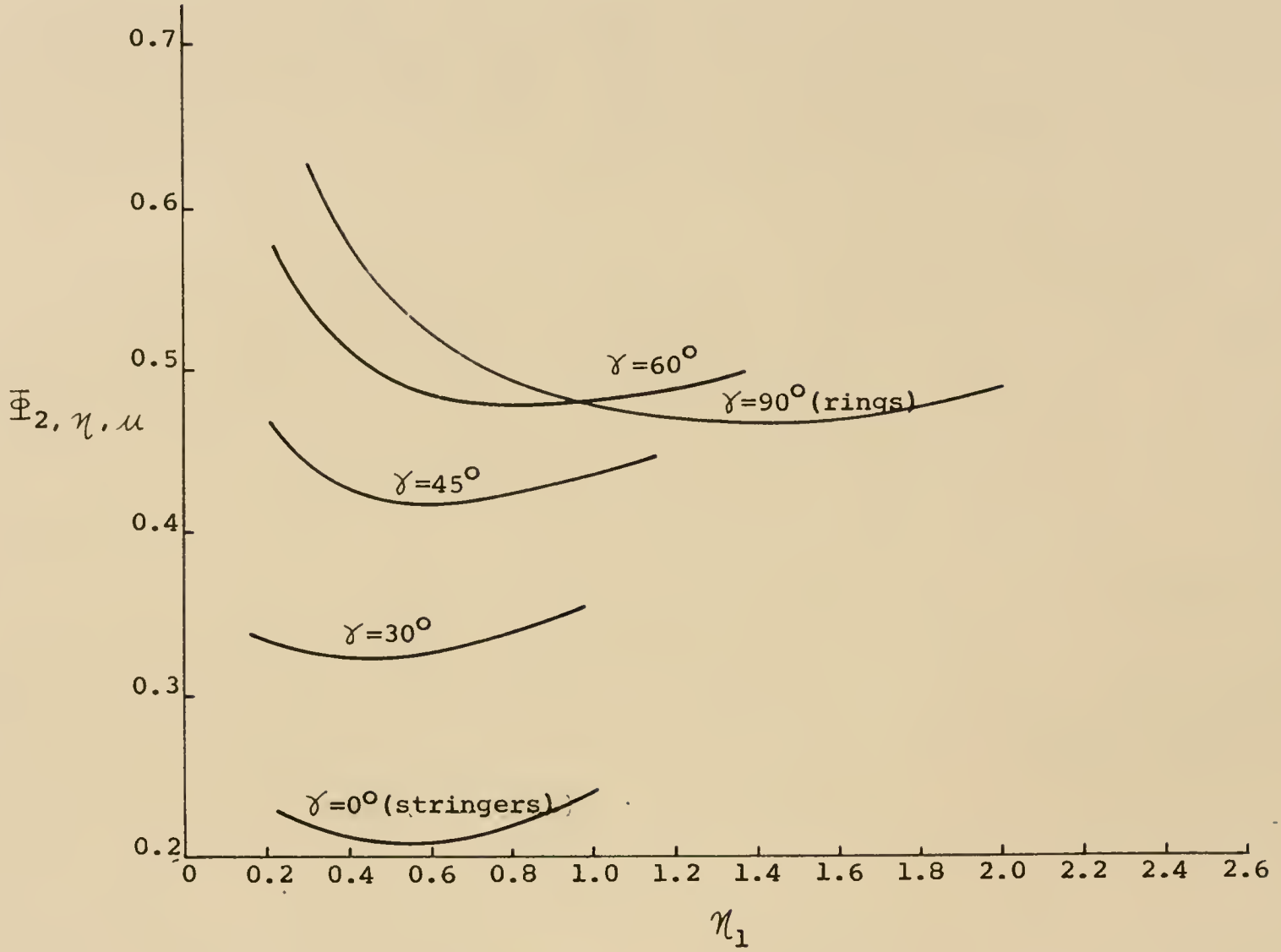

Fig. 12. Minimum Stress Parameter $\Phi_{2,\eta,\mu}$ as a Function of Deflection η_1 at Different Inclined Angles.

($\overline{E}\ \overline{I}\ \overline{\ell}$ = 2 , K = 0 , Γ = 0 , $\overline{p}$ = 0)

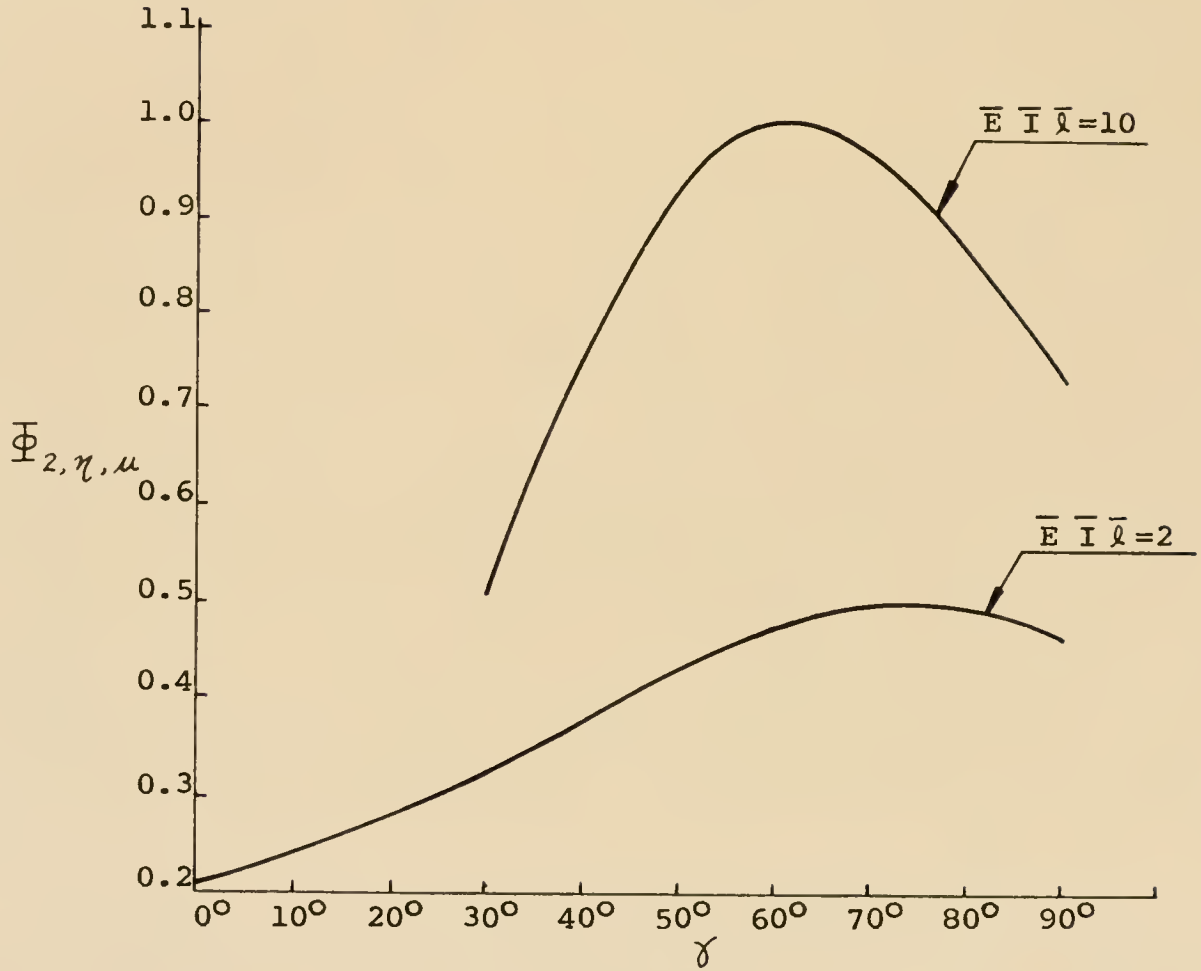

Fig. 13. Relation Between Minimum Stress Parameter, $\Phi_{2,\eta,\mu}$ and Inclined Angles
($K = 0$, $\Gamma = 0$, $\bar{p} = 0$)

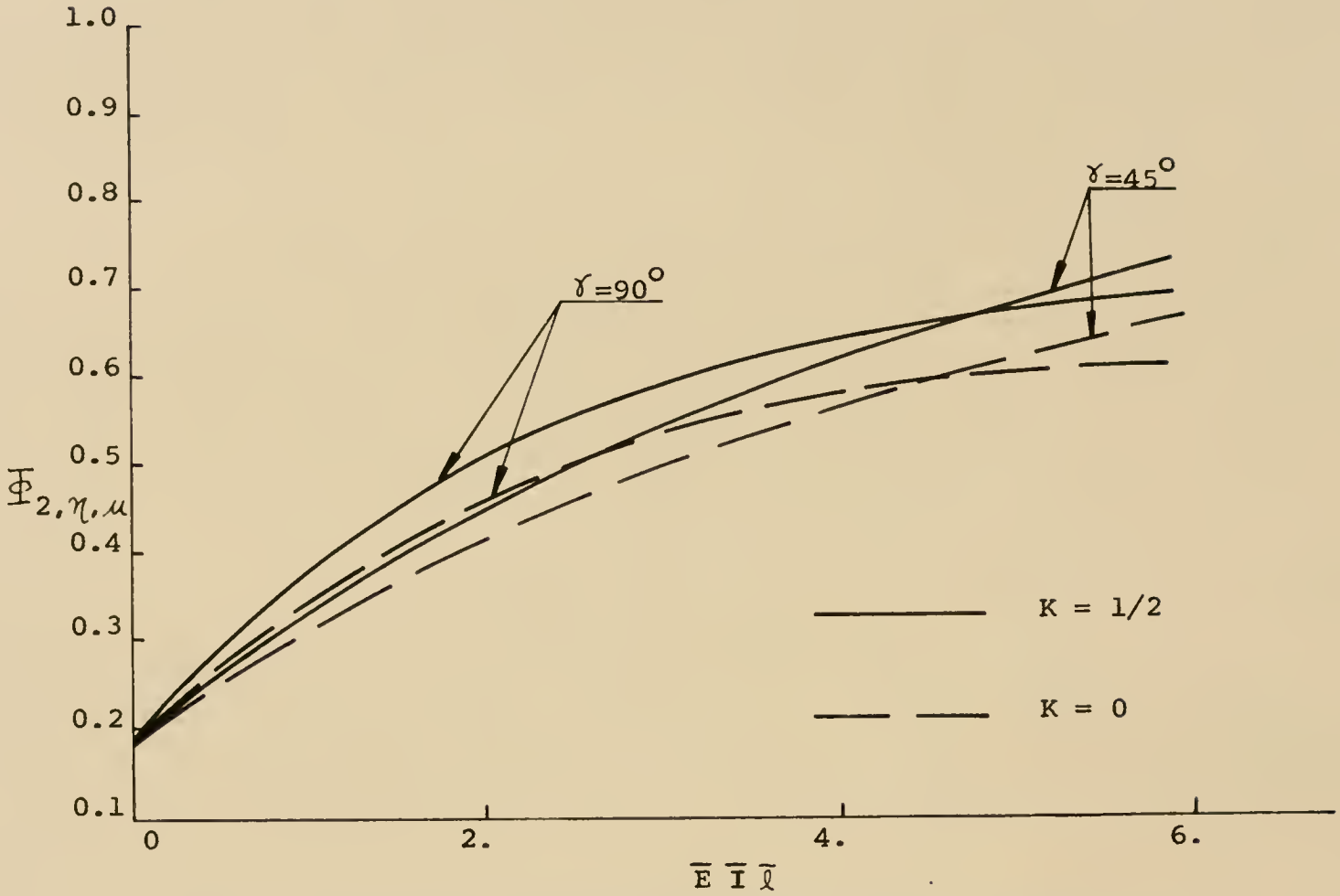

Fig. 14. Relation Between Minimum Stress Parameter $\Phi_{2,\eta,\mu}$ and Rigidity of the Stiffeners.

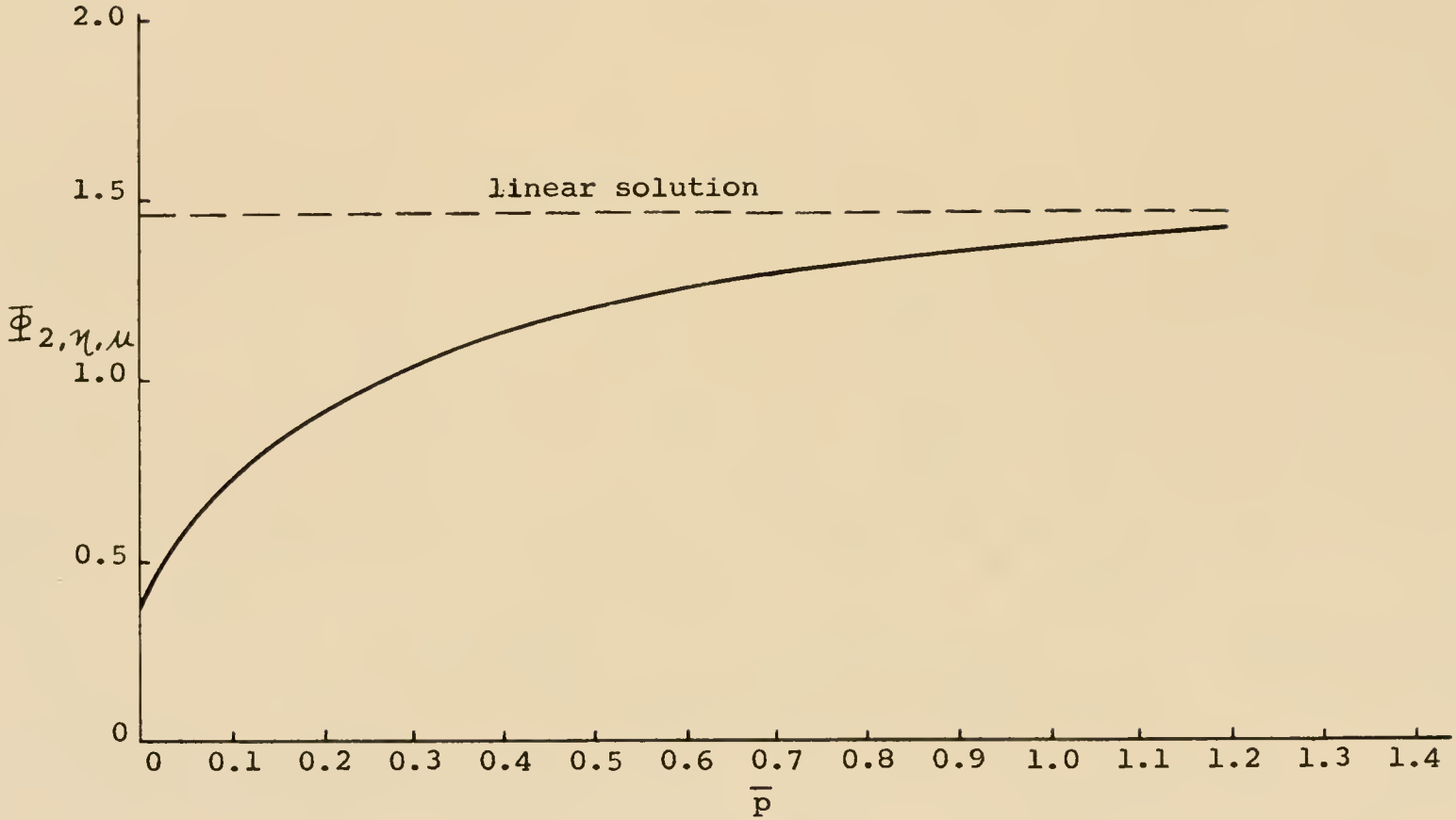

Fig. 15. Relation Between Minimum Stress Parameter $\Phi_{2,\eta,\mu}$ and Internal Pressure $\bar{p}$.

($\gamma = 45^{\circ}$, $\bar{E}\,\bar{I}\,\bar{\ell} = 2$, $K = 0$, $\Gamma = 0$)

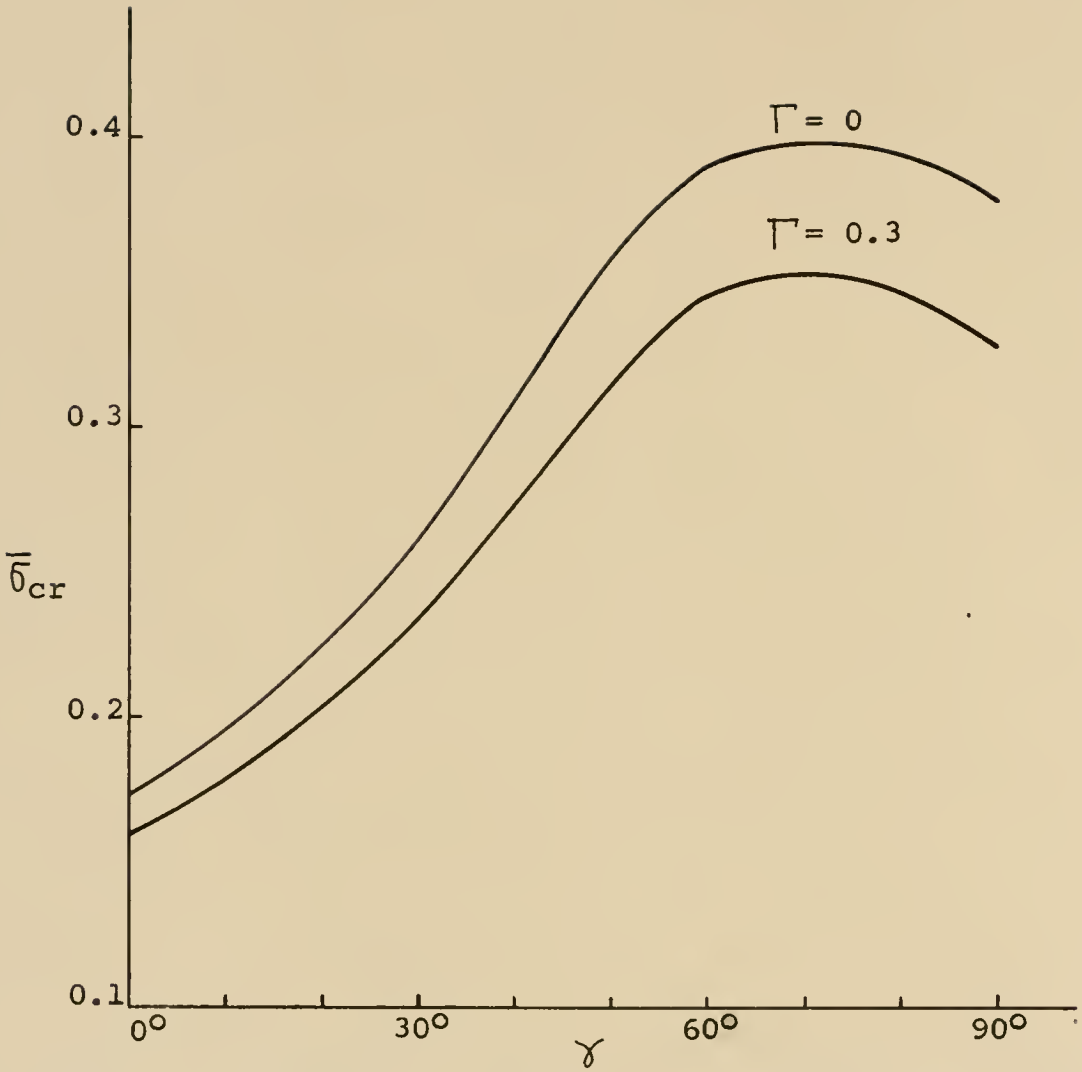

Fig. 16. Comparison of Effect of the Imperfection Ratio on the Stiffened Shells Under Axial Compression

$(\bar{E}\ \bar{I}\ \bar{\ell} = 2\ ,\ K = 0\ ,\ \bar{p} = 0)$

Fig. 17. Typical Buckling Patterns for Unpressurized-Stiffened Shell Under Axial Compression

(R = 4 in. t = 0.0075 in. t_1 = 0.02 in.)

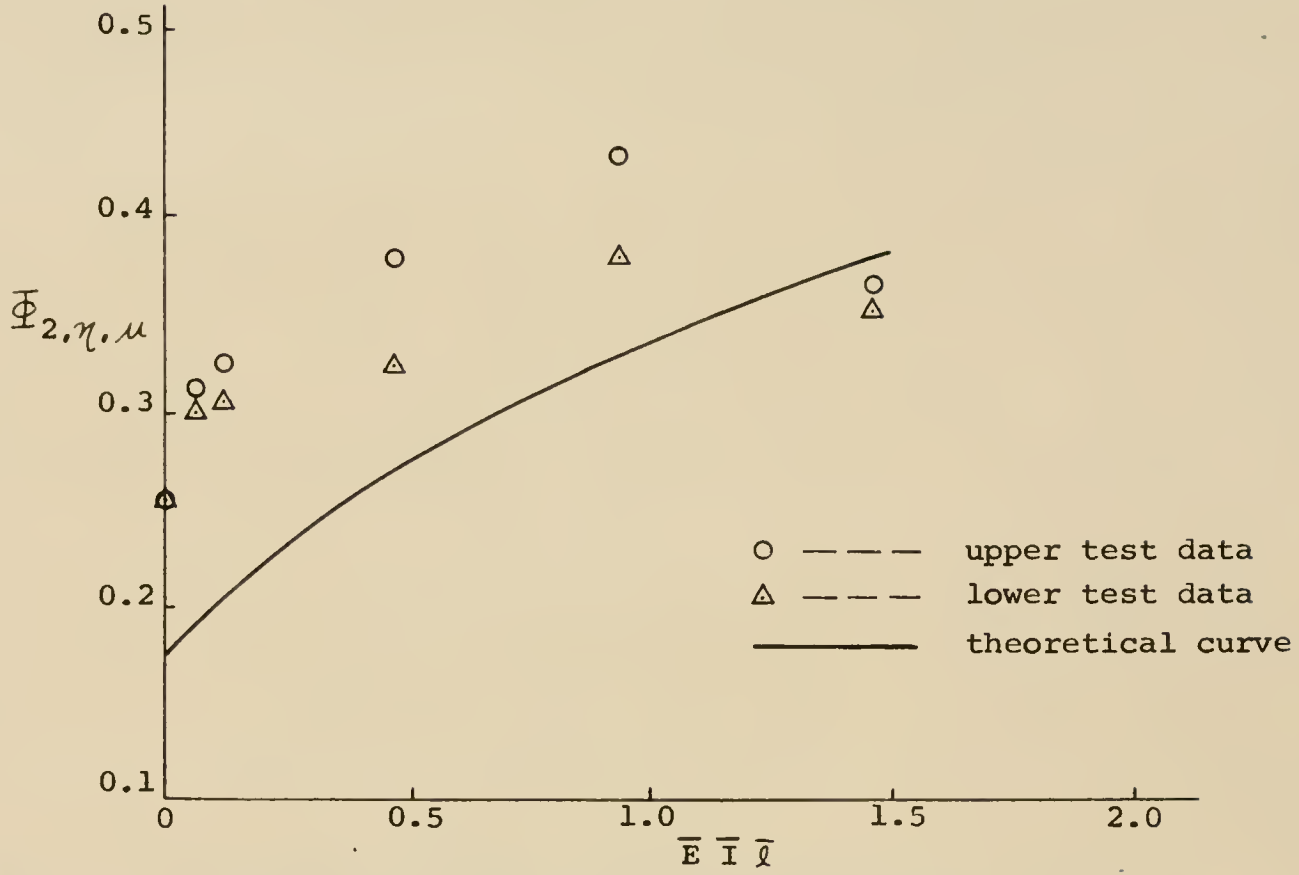

Fig. 18. Comparison of Theoretical and Experimental Results on the Stiffened Shells Under Pure Bending

($\gamma = 45^{\circ}$, K = 0 , $\Gamma = 0$, $\bar{p} = 0$)

APPENDICES

APPENDIX A

APPENDIX A

ENERGY R_i IN STIFFENERS

To neglect the energy terms R_1, R_2, R_3 and R_4 in Eq. (37), we may refer to Ref. (34). In that study, the numerical results have indicated that the minimum stress is only slightly affected by these terms. Also, it is to be noted that the minimum stress is nearly independent of the locations of the stiffeners. In the present analysis and experimental results, it indicates that the shells buckle in multiple waves pattern. This implies that m^2 and n^2 are much greater than unity. Moreover, from the experiment the buckling stress is not affected by small change in the stiffeners' locations. Thus, the summations of sine functions of the energy of the stiffeners may be assumed very small when compared with the constant terms. The approximate solution can be much simplified by neglecting these R_i terms (i = 1, 2, 3, 4). However, the expressions for R_1, R_2, R_3 and R_4 are expressed below for the purpose of reference.

$$R_1 = \frac{(1-\Gamma)^2}{\rho^2} \sum_{k=1}^{N_k} \frac{\bar{E}_k \bar{I}_k}{2} \left\{ \frac{\bar{b}_2^2}{4} (C_1 + u C_2)^2 (C_1 - u C_2)^2 \times \right.$$

$$\times \left[\frac{R}{L 2mC_1} \sin\left(2mC_1 \frac{l_k}{R}\right) + \frac{R}{L 2nC_2} \sin\left(2nC_2 \frac{l_k}{R}\right) \right]$$

$$+ 2\bar{b}_2 \bar{b}_3 u^2 (C_1 + uC_2)^2 C_2^2 \left[\frac{R}{L(mC_1 - nC_2)} \sin(mC_1 - nC_2)\left(\frac{l_k}{R}\right) \right.$$

$$\left. + \frac{R}{L(mC_1 + 3nC_2)} \sin(mC_1 + 3nC_2)\left(\frac{l_k}{R}\right) \right] + 2\bar{b}_2 \bar{b}_4 C_1^2 \times$$

$$\times (C_1 + uC_2)^2 \left[\frac{R}{L(3mC_1 + nC_2)} \sin(3mC_1 + nC_2)\left(\frac{l_k}{R}\right) \right.$$

$$\left. + \frac{R}{L(mC_1 - nC_2)} \sin(mC_1 - nC_2)\left(\frac{l_k}{R}\right) \right] + 2\bar{b}_2 \bar{b}_3 u^2 (C_1 - uC_2) C_2^2 \times$$

$$\times \left[\frac{R}{L(mC_1 - 3nC_2)} \sin(mC_1 - 3nC_2)\left(\frac{l_k}{R}\right) + \frac{R}{L(mC_1 + nC_2)} \sin(mC_1 + nC_2)\left(\frac{l_k}{R}\right) \right]$$

$$+ 2\bar{b}_2 \bar{b}_4 C_1^2 (C_1 - uC_2)^2 \times \left[\frac{R}{L(3mC_1 - nC_1)} \sin(3mC_1 - nC_2)\left(\frac{l_k}{R}\right) \right.$$

$$\left. + \frac{R}{L(mC_1 + nC_2)} \sin(mC_1 + nC_2)\left(\frac{l_k}{R}\right) \right] + 16\bar{b}_3 \bar{b}_4 u^2 C_1^2 C_2^2 \left[\frac{R}{2L(mC_1 + nC_2)} \times \right.$$

$$\left. \times \sin(2mC_1 + 2nC_2)\left(\frac{l_k}{R}\right) + \frac{R}{2L(mC_1 - nC_2)} \sin 2(mC_1 - nC_1)\left(\frac{l_k}{R}\right) \right]$$

$$+ \frac{\bar{b}_2^2}{8} \left[(C_1 + uC_2)^4 \frac{R}{2L(mC_1 + uC_2)} \sin 2(mC_1 + nC_2)\left(\frac{l_k}{R}\right) + \right.$$

$$+(C_1-uC_2)^4\ \frac{R}{2L(mC_1-nC_2)}\ \sin 2(mC_1-nC_2)\left(\frac{l_k}{R}\right)\Big]+2\bar{b}_3^{\,2}u^4C_2^{\,4}\ \frac{R}{LnC_2}\times$$

$$\times\sin(4nC_2)\left(\frac{l_k}{R}\right)+2\bar{b}_4^{\,2}C_1^{\,4}\ \frac{R}{LnC_2}\ \sin(4nC_2)\left(\frac{l_k}{R}\right)\Big\}$$

$$R_2=\frac{(1-\Gamma^2)}{\beta^2}\sum_{j=1}^{N_j}\frac{\bar{E}_j\bar{I}_j}{2}\Big\{\frac{\bar{b}_2^{\,2}}{4}(C_3+uC_4)^2(C_3-uC_4)^2\times\Big[\frac{R}{2LmC_3}\sin 2mC_3\left(\frac{l_j}{R}\right)$$

$$+\frac{R}{2LnC_4}\ \sin 2nC_4\left(\frac{l_j}{R}\right)\Big]+2\bar{b}_2\bar{b}_3u^2(C_3+uC_4)^2C_4^{\,2}\Big[\frac{R}{L(mC_3-nC_4)}\times$$

$$\times\sin(mC_3-nC_4)\left(\frac{l_j}{R}\right)+\frac{R}{L(mC_3+3nC_4)}\ \sin(mC_3+3nC_4)\left(\frac{l_j}{R}\right)\Big]$$

$$+2\bar{b}_2\bar{b}_4C_3^{\,2}(C_3+uC_4)^2\Big[\frac{R}{L(3mC_3+nC_4)}\sin(3mC_3+nC_4)\left(\frac{l_j}{R}\right)$$

$$+\frac{R}{L(mC_3-nC_4)}\ \sin(mC_3-nC_4)\left(\frac{l_j}{R}\right)\Big]+2\bar{b}_2\bar{b}_3u^2(C_3-uC_4)^2C_4^{\,2}\times$$

$$\times\Big[\frac{R}{L(mC_3-3nC_4)}\ \sin(mC_3-3nC_4)\left(\frac{l_j}{R}\right)+\frac{R}{L(mC_3+nC_4)}\ \sin(mC_3+nC_4)\left(\frac{l_j}{R}\right)\Big]$$

$$+2\bar{b}_2\bar{b}_4(C_3-uC_4)^2C_3^2\Big[\frac{R}{L(3mC_3-nC_4)}\sin(3mC_3-nC_4)\left(\frac{l_j}{R}\right)$$

$$+\frac{R}{L(mC_3+nC_4)}\ \sin(mC_3+nC_4)\left(\frac{l_j}{R}\right)\Big]+16\bar{b}_3\bar{b}_4u^2C_3^{\,2}C_4^{\,2}\Big[\frac{R}{2L(mC_3+nC_4)}\times$$

$$\times\sin 2(mC_3+nC_4)\left(\frac{l_j}{R}\right)+\frac{R}{2L(mC_3-nC_4)}\ \sin 2(mC_3-nC_4)\left(\frac{l_j}{R}\right)$$

$$+\frac{\bar{b}_2^{\,2}}{8}\Big[(C_3+uC_4)^4\ \frac{R}{2L(mC_3+nC_4)}\ \sin 2(mC_3+nC_4)\left(\frac{l_j}{R}\right)+$$

$$+(C_3-\mu C_4)^4\frac{R}{2L(mC_3-nC_4)}\sin 2(mC_3-nC_4)\left(\frac{l_j}{R}\right)\Big]+2\bar{b}_3^{\,2}\mu^4C_4^{\,4}\frac{R}{LnC_4}\times$$

$$\times\sin(4nC_4)\left(\frac{l_j}{R}\right)+2\bar{b}_4^{\,2}C_3^{\,4}\frac{R}{nLC_4}\sin\frac{4nC_4}{R}l_j\Big\}$$

$$R_3=\frac{(1-\Gamma)^2}{\beta^2}\sum_{k=1}^{N_k}\frac{\bar{G}_k\bar{J}_k}{2}\left\{\frac{\bar{b}_2^{\,2}}{8}\left[\frac{R}{2L(mC_1+nC_2)}\sin\frac{2(mC_1+nC_2)}{R}l_k\right.\right.$$

$$+\frac{R}{2L(mC_1-nC_2)}\sin 2(mC_1-nC_2)\left(\frac{l_k}{R}\right)+2(C_1^2-\mu C_2^2)(C_2^2-\mu^2C_1^2)\times$$

$$\times\left(\frac{R}{2LmC_1}\sin\frac{2mC_1}{R}l_k+\frac{R}{2LnC_2}\sin(2nC_2)\left(\frac{l_k}{R}\right)\right)\Big]+2C_1^2C_2^2\times$$

$$\times\Big[\mu^4\bar{b}_3^{\,2}\frac{R}{LnC_3}\sin 4nC_2\left(\frac{l_k}{R}\right)+\bar{b}_4^{\,2}\frac{R}{LmC_1}\sin 4mC_1\left(\frac{l_k}{R}\right)\Big]-2\mu^2\bar{b}_2\bar{b}_3C_1C_2\times$$

$$\times\Big[(C_1+\mu C_2)(C_2-\mu C_1)\Big(\frac{R}{L(mC_1+nC_2)}\sin(mC_1+nC_2)\left(\frac{l_k}{R}\right)$$

$$+\frac{R}{L(mC_1-nC_2)}\sin(mC_1-nC_2)\frac{l_k}{R}\Big)+(C_1-\mu C_2)(C_2+\mu C_1)\Big(\frac{R}{L(mC_1+nC_2)}\times$$

$$\times\sin(mC_1+nC_2)\left(\frac{l_k}{R}\right)+\frac{R}{L(mC_1-3nC_2)}\sin(mC_1-3nC_2)\left(\frac{l_k}{R}\right)\Big)\Big]$$

$$+2C_1C_2\bar{b}_2\bar{b}_4\Big[(C_1-\mu C_2)(C_2-\mu C_1)\Big(\frac{R}{L(3mC_1+nC_2)}\sin(3mC_1+nC_2)\left(\frac{l_k}{R}\right)$$

$$+\frac{R}{L(mC_1-nC_2)}\sin(mC_1-nC_2)\left(\frac{l_k}{R}\right)\Big)+(C_1-\mu C_2)(C_2+\mu C_1)\Big(\frac{R}{L(3mC_1-nC_2)}\times$$

$$\times\sin(3mC_1-nC_2)\left(\frac{l_k}{R}\right)+\frac{R}{L(mC_1+nC_2)}\sin(mC_1+nC_2)\left(\frac{l_k}{R}\right)\Big)\Big]+$$

$$-16\,u^2\bar{b}_3\bar{b}_4 C_1^2 C_2^2\left[\frac{R}{2L(mC_1+nC_2)}\sin 2(mC_1+nC_2)\left(\frac{l_k}{R}\right)\right.$$

$$\left.+\frac{R}{2L(mC_1-nC_2)}\sin 2(mC_1-nC_2)\left(\frac{l_k}{R}\right)\right]\Bigg\}$$

$$R_4=\frac{(1-\Gamma)^2}{\beta^2}\cdot\sum_{j=1}^{N_j}\frac{\bar{G}_j\bar{J}_j}{2}\left\{\frac{\bar{b}_2}{8}^2\left[\frac{R}{2L(mC_3+nC_4)}\sin 2(mC_3+nC_4)\left(\frac{l_j}{R}\right)\right.\right.$$

$$\left.+\frac{R}{2L(mC_3-nC_4)}\sin 2(mC_3-nC_4)\left(\frac{l_j}{R}\right)+2(C_3^2-u^2C_4^2)(C_4^2-u^2C_3^2)\times\right.$$

$$\times\left(\frac{R}{2L(mC_3)}\sin\frac{2mC_3}{R}l_j+\frac{R}{2LnC_4}\sin 2nC_4\left(\frac{l_j}{R}\right)\right)\Big]+2C_3^2C_4^2\times$$

$$\times\left(\bar{b}_3^2u^4\frac{R}{nLC_4}\sin 4nC_4\left(\frac{l_j}{R}\right)+\bar{b}_4^2\cdot\frac{R}{mLC_3}\sin 4mC_3\left(\frac{l_j}{R}\right)\right)$$

$$-2u^2\bar{b}_2\bar{b}_3C_3C_4\left[(C_3+uC_4)(C_4-uC_3)\left(\frac{R}{L(mC_3+nC_4)}\times\right.\right.$$

$$\left.\times\sin(mC_3+nC_4)\left(\frac{l_j}{R}\right)+\frac{R}{L(mC_3-nC_4)}\sin(mC_3-nC_4)\left(\frac{l_j}{R}\right)\right)$$

$$+(C_3-uC_4)(C_4+uC_3)\left(\frac{R}{L(mC_3+nC_4)}\sin(mC_3+nC_4)\left(\frac{l_j}{R}\right)\right.$$

$$\left.\left.+\frac{R}{L(mC_3-3nC_4)}\sin(mC_3-3nC_4)\left(\frac{l_j}{R}\right)\right)\right]+2C_3C_4\bar{b}_2\bar{b}_4\times$$

$$\times\left[(C_3+uC_4)(C_4-uC_3)\left(\frac{R}{L(3mC_3+nC_4)}\sin(3mC_3+nC_4)\left(\frac{l_j}{R}\right)\right.\right.$$

$$\left.\left.+\frac{R}{L(mC_3-nC_4)}\sin(mC_3-nC_4)\left(\frac{l_j}{R}\right)\right)+(C_3-uC_4)(C_4+uC_3)\times\right.$$

$$\times\left(\frac{R}{L(3mc_3-nc_4)}\sin(3mc_3-nc_4)\left(\frac{l_j}{R}\right)+\frac{R}{L(mc_3+nc_4)}\times\right.$$

$$\left.\times\sin(mc_3+nc_4)\left(\frac{l_j}{R}\right)\right]-16\mu^2\bar{b}_3\bar{b}_4c_3^2c_4^2\left(\frac{R}{2L(mc_3+nc_4)}\times\right.$$

$$\left.\times\sin 2(mc_3+nc_4)\left(\frac{l_j}{R}\right)+\frac{R}{2L(mc_3-nc_4)}\sin 2(mc_3-nc_4)\left(\frac{l_j}{R}\right)\right)\Bigg\}$$

APPENDIX B

APPENDIX B
COMPUTER PROGRAM I
STIFFENED CYLINDRICAL SHELLS UNDER AXIAL COMPRESSION

```
    1 READ INPUT TAPE 5, 10,E,G,C,D,Q,R,H,P,II,ID,IF,JI,JD,J
      1F,KI,KD,KF
   10 FORMAT (8F5.3,9I4)
      DO 50 K=KI,KF,KD
      Z=.01*FLOATF(K)
      DO 50 I=II,IF,ID
      X=.01*FLOATF(I)
      DO 50 J=JI,JF,JD
      Y=.001*FLOATF(J)
      YS=Y**2
      XS=X**2
      XQ=XS**2
      CS=C**2
      CQ=CS**2
      DS=D**2
      DQ=DS**2
      QS=Q**2
      QQ=QS**2
      RS=R**2
      RQ=RS**2
      HM=1.-H
      HP=1.+H
      HMS=1./HM**2
      S1=E*(CQ+QQ+XQ*(DQ+RQ)+6.*XS*(CS*DS+QS*RS)+G*(((C+X*D)
     1*(D-X*C))**2+((C-X*D)*(D+X*C))**2+((Q+X*R)*(R-X*Q))**2
     2+((Q-X*R)*(R+X*Q))**2)/2.)/4.
      S2=E*XQ*(DQ+RQ+G*(CS*DS+QS*RS))
      S3=E*(CQ+QQ+G*(CS*DS+QS*RS))
      G1=1./(1.+XS)**2
      G2=1./(9.+XS)**2
      G3=1./(1.+9.*XS)**2
      A1=3.*(1.+XS)**2/32.+S1
      A3=-(2.*(2.+H)*(1.+Z)*G1+Z/2.)*XS
      A4=HP*4.*XQ*(G1*(1.+Z)**2+G2*Z**2+G3)
      A5=HP*(1.+XQ)/16.
      B1=3.*XQ/8.+S2
      B4=HP*2.*XQ*G1*Z**2
      B5=HP*XQ*.5*(G3+(1.+Z)*G1)
      B6=-XS*.25*G1
      C1=3./8.+S3
      C4=HP*2.*XQ*G1
      C5=HP*XQ*.5*(G2+(1.+1./Z)*G1)
      C6=-XS*(G1+(1.+H)/8.)*.25/Z
      H1=C5+C6/Y-A5
      H2=B5+B6/Y
      D2=A1*H2-B1*A5
      D3=(G1+A3*Y+A4*YS)*H2-B4*A5*YS
      F2=A1*(C5+C6/Y)-C1*A5
      F3=(G1+A3*Y+A4*YS)*(C5+C6/Y)-A5*(.25+C4*YS)
```

```
      W1=(D2*D3*H1*H1/F3**2+F2*H2*H2/F3-H2*H1*(F2*D3/F3+D2)/
     1F3)*HMS
      W2=-HMS*3*XS*P*(D2*D3*H1*(H1+A5)/F3**2+F2*H2*(H2-A5)/F
     13-(2.*H2*(H1+A5)+A5*A5-H2*A5-(H1+A5)*A5)*.5*(F2*D3/F3+
     2D2)/F3)
      W3=HMS*2.25*XQ*P*P*(D2*D3*(H1+A5)**2/F3**2+F2*(H2-A5)*
     1*2/F3-(H1+A5)*(H2-A5)*(F2*D3/F3+D3)/F3)+D2*D2+(D3*F2/F
     23)**2-2.*D2*D3*F2/F3
      DISC=W2**2-4.*W1*W3
      IF (DISC) 50, 60, 70
60    X1R=-W2/(2.*W1)
      X2R=X1R
      GO TO 80
70    S=SQRTF(DISC)
      X1R=(-W2+S)/(2.*W1)
      X2R=(-W2-S)/(2.*W1)
      GO TO 80
80    WRITE OUTPUT TAPE 6, 20, Z,X,Y,X1R,X2R,P,W1,W2,W3,E
20    FORMAT (10F8.3)
50    CONTINUE
      GO TO 1
      END
```

Symbols Used In Computer Program I

E =	$\bar{E}\,\bar{I}\,\bar{\ell}$	G =	K
C =	C_1	D =	C_2
Q =	C_3	R =	C_4
H =	Γ	P =	$\bar{p}$
Z =	η_1	x =	μ
Y =	η	X2R =	$\bar{\sigma}_c$

COMPUTER PROGRAM II
STIFFENED CYLINDRICAL SHELLS
UNDER BENDING OR TRANSVERSE SHEAR

```
    1 READ INPUT TAPE 5, 10,E,G,C,D,Q,R,H,P,II,ID,IF,JI,JD,J
      1F,KI,KD,KF
   10 FORMAT (8F5.3,9I4)
      DO 50 K=KI,KF,KD
      Z=.01*FLOATF(K)
      DO 50 I=II,IF,ID
      X=.01*FLOATF(I)
      DO 50 J=JI,JF,JD
      Y=.001*FLOATF(J)
      ZS=Z**2
      YS=Y**2
      XS=X**2
      XQ=XS**2
      CS=C**2
      CQ=CS**2
      DS=D**2
      DQ=DS**2
      QS=Q**2
      QQ=QS**2
      RS=R**2
      RQ=RS**2
      HM=1.-H
      HP=1.+H
      HMS=1./HM**2
      S1=3.*E*(CQ+QQ+XQ*(DQ+RQ)+6.*XS*(CS*DS+QS*RS)+G*(((C+X
     1*D)*(D-X*C))**2+((C-X*D)*(D+X*C))**2+((Q+X*R)*(R-X*Q))
     2**2+((Q-X*R)*(R+X*Q))**2)/2.)/8.
      S2=1.5*E*XQ*(DQ+RQ+G*(CS*DS+QS*RS))
      S3=1.5*E*(CQ+QQ+G*(CS*DS+QS*RS))
      G1=1./(1.+XS)**2
      G2=1./(9.+XS)**2
      G3=1./(1.+9.*XS)**2
      A1=9.*(1.+XS)**2/64.+S1
      A3=-(1.5*(2.+H)*(1.+Z)*G1+3.*Z/8.)*XS
      A4=HP*9.*XQ*(G1*(1.+Z)**2+G2*ZS+G3)/4.
      A5=HP*9.*(1.+XQ)/256.
      B1=9.*XQ/16.+S2
      B4=HP*9.*XQ*G1*ZS/8.
      B5=HP*9.*XQ*((1.+Z)*G1+G3)/32.
      B6=-(3.*XS*G1)/16.
      C1=9./16.+S3
      C4=HP*9.*XQ*G1/8.
      C5=HP*9.*XQ*((1.+1./Z)*G1+G2)/32.
      C6=-3.*XS*(HP/8.+G1)/(16.*Z)
      H1=C5+C6/Y-A5
      H2=B5+B6/Y
      D2=A1*H2-B1*A5
      D3=(G1+A3*Y+A4*YS)*H2-B4*A5*YS
      F2=A1*(C5+C6/Y)-C1*A5
```

```
      F3=(G1+A3*Y+A4*YS)*(C5+C6/Y)-A5*(.25+C4*YS)
      W1=HMS*.25*(D2*D3*H1*H1/F3**2+F2*H2*H2/F3-H1*H2*(F2*D3
     1/F3+D2)/F3)
      W2=-HMS*1.5*XS*P*(D2*D3*H1*(H1+A5)/F3**2+F2*H2*(H2-A5)
     1/F3-(2.*H2*(H1+A5)+A5*A5-H2*A5-(H1+A5)*A5)*.5*(F2*D3/F
     23+D2)/F3)
      W3=HMS*2.25*XQ*P*P*(D2*D3*(H1+A5)**2/F3**2+F2*(H2-A5)*
     1*2/F3-(H1+A5)*(H2-A5)*(F2*D3/F3+D3)/F3)+D2*D2+(D3*F2/F
     23)**2-2.*D2*D3*F2/F3
      DISC=W2**2-4.*W1*W3
      IF (DISC) 50, 60, 70
60    X1R=-W2/(2.*W1)
      X2R=X1R
      GO TO 80
70    S=SQRTF(DISC)
      X1R=(-W2+S)/(2.*W1)
      X2R=(-W2-S)/(2.*W1)
      GO TO 80
80    WRITE OUTPUT TAPE 6, 20, Z,X,Y,X1R,X2R,P,W1,W2,W3,E
20    FORMAT (10F8.3)
50    CONTINUE
      GO TO 1
      END
```

Symbols Used In Computer Program II

E = $\bar{E}\,\bar{I}\,\bar{\ell}$ G = K

C = C_1 D = C_2

Q = C_3 R = C_4

H = Γ P = $\bar{p}$

Z = η_1 x = μ

Y = η X2R = $2\,\bar{\Phi}_2 = 2(\bar{\sigma}_b + 3/2\,\bar{\sigma})$ or

(X2R = $2\,\bar{\Phi}_3 = \bar{P}$ for transverse load)

BIBLIOGRAPHY

1. W. Fairbairn, "On the Resistance of Tubes to Collapse," Phil. Trans. Roy. Soc., Vol. 148, pp. 389-413, 1859.

2. G. H. Bryan, "On the Stability of Elastic Systems," Proceedings of the Cambridge Philosophical Society, Vol. 6, Part 4, pp. 199-211, 1888.

3. A. E. H. Love, A Treatise on the Mathematical Theory of Elasticity, fourth Edition. Reprinted in the U.S.A., by Dover Publication, New York, N. Y., 1944.

4. S. Timoshenko, and J. Gore, Theory of Elastic Stability, McGraw-Hill Book Company, New York, N. Y., 1961.

5. R. V. Southwell, "On the General Theory of Elastic Stability," Phil. Trans. Roy. Soc., Series A, pp. 187-213, 1914.

6. L. H. Donnell, "Stability of Thin-Walled Tubes under Torsion," NACA Report 479, 1933.

7. S. B. Batdorf, "A Simplified Method of Elastic-Stability Analysis for Thin Cylindrical Shells," NACA Report 874, 1947.

8. H. S. Suer, and L. A. Harris, "The Stability of Thin-Walled Cylinders under Combined Torsion and External Lateral or Hydrostatic Pressure," Journal of Applied Mechanics, Vol. 81, Series E., No. 1, pp. 138-139, 1959.

9. P. Seide, and V. I. Weingartern, "On the Buckling of Circular Cylindrical Shells Under Pure Bending," Journal of Applied Mechanics, Vol. 28, No. 1, pp. 112-116, March, 1961.

BIBLIOGRAPHY (Continued)

10. L. H. Donnell, "A New Theory for the Buckling of Thin Cylinders Under Axial Compression and Bending," ASME Transactions, Vol. 56, pp. 795-806, 1934.

11. Th. von Karman, and H. S. Tsien, "The Buckling of Thin Cylindrical Shells under Axial Compression," Journal of the Aeronautical Sciences, Vol. 8, pp. 303-312, 1941.

12. J. Kempner, "Postbuckling Behavior of Axially Compressed Circular Cylindrical Shells," Journal of the Aeronautical Sciences, Vol. 21, pp. 329-335, 1954.

13. R. E. Ekstrom, "Theoretical and Experimental Investigation of the Buckling of Thin Cylindrical Shells Subject to Combined Torsion and Uniform External Pressure," University of Florida, Dissertation, 1960.

14. S. Y. Lu, and W. A. Nash, "Elastic Instability of Pressurized Cylindrical Shells under Compression or Bending," Proc. 4th U.S. Congr. Appl. Mechanics, Vol. 1, pp. 18-21, 1962.

15. W. F. Thielemann, "New Development in the Non-Linear Theory of the Buckling of Thin Cylindrical Shells," Report by Deutsche Versuchsanstalt fur Luftfahrt E. V., Aeronautics and Astronautics, Pergamon Press, New York, 1960.

16. E. H. Dill, "General Theory of Large Deflections of Thin Shells," NASA TN, D-826, March, 1961.

17. L. H. Donnell, and C. C. Wan, "Effect of Imperfections on Buckling of Thin Cylinders and Columns uhder Axial Compression," Journal of Applied Mechanics, Vol. 17, No. 1, 1950.

18. T. T. Loo, "Effects of Large Deflections and Imperfections on the Elastic Buckling of Cylinders under Torsion and Axial Compression," Proc. 2nd U.S. Congr. Appl. Mechanics, 1954.

BIBLIOGRAPHY (Continued)

19. L. H. N. Lee, "Effects of Modes of Initial Imperfections on the Stability of Cylindrical Shells under Axial Compression," University of Notre Dame, NASA TN D-1510, pp. 143-158, December, 1962.

20. W. A. Nash, "Effect of Large Deflections and Initial Imperfections on the Buckling of Cylindrical Shells Subject to Hydrostatic Pressure," Journal of Aeronautical Sciences, Vol. 22, No. 4, April, 1955.

21. W. A. Nash, "Buckling of Initially Imperfect Cylindrical Shells Subject to Torsion," Journal of Applied Mechanics, Vol. 79, pp. 125-130, March, 1957.

22. S. Y. Lu, and W. A. Nash, "Buckling of Initially Imperfect Axially Compressed Cylindrical Shells," NASA TN D-1510, pp. 187-202, December, 1962.

23. W. A. Nash, "General Instability of Ring-Reinforced Cylindrical Shells Subject to Hydrostatic Pressure," Journal of Aeronautical Sciences, Vol. 22, No. 4, April, 1955.

24. N. A. Alfutov, "Stability of Cylindrical Shells Reinforced with Transverse Stiffening Ring and Subject to Uniform External Pressure," Inzh. Sborn., Vol. 23, pp. 36-46, 1956.

25. K. I. McKenzie, "The Buckling of a Pressurized Stiffened Cylinder under Axial Load," Royal Aircraft Establishment, Report No. Structures-247, 1959.

26. S. N. Kan and D. Ye. Lipovskiy, "Longitudinal-Transverse Bending of Stiffened Circular Cylindrical Shells," NASA TTF-194, April, 1964.

BIBLIOGRAPHY (Continued)

27. G. D. Galletly, R. C. Slankard and E. Wenk, Jr., "General Instability of Ring-Stiffened Cylindrical Shells Subject to External Hydrostatic Pressure - A Comparison of Theory and Experiment," Presented at I X International Congress of Applied Mechanics (Brussels), 1956.

28. J. M. Hedgepeth and D. B. Hall, "Stability of Stiffened Cylinders," The Martin Company, Baltimore, Maryland AIAA Paper, No. 65-79, January, 1965.

29. H. Becker and G. Gerard, "Elastic Stability of Orthotropic Shells," Journal of the Aerospace Sciences, Vol. 29, No. 5, pp. 505-512, May, 1962.

30. N. J. Huffington, Jr., "Theoretical Determination of Rigidity Properties of Orthogonally Stiffened Plates," Journal of Applied Mechanics, Vol. 23, No. 3, March, 1956.

31. Arie van der Neut, "General Instability of Orthogonally Stiffened Cylindrical Shells," Aeronautical Department, Technological University, Delft, (Netherlands), NASA TN D-1510, pp. 309-319, December, 1962.

32. H. Becker, "General Instability of Stiffened Cylinders," NACA TN 4237, July, 1958.

33. D. L. Block, "Influence of Ring Stiffeners on Instability of Orthotropic Cylinders in Axial Compression," NASA TN D-2482, 1964.

34. R. L. Lee, "Stability of Pressurized Ring-Stiffened Cylindrical Shells Subject to Axial Compression," University of Florida, Thesis, June, 1962.

35. J. C. MaCoy, "An Experimental Investigation of the General Instability of Ring-Stiffened Unpressurized, Thin-Walled Cylinders under Axial Compression," California Institute of Technology, California, 1958.

BIBLIOGRAPHY (Continued)

36. J. P. Peterson, and M. B. Dow, "Bending and Compression Tests of Pressurized Ring-Stiffened Cylinders," NASA TN D-360, April, 1960.

37. E. Lundquist, "Strength Tests of Thin-Walled Duralumin Cylinders in Combined Transverse Shear and Bending," NACA Technical Note No. 523, April, 1935.

38. L. A. Harris, H. S. Suer, W. T. Skene, and R. J. Benjamin, "The Stability of Thin-Walled Unstiffened Circular Cylinders under Axial Compression Including the Effects of Internal Pressure," Journal of the Aeronautical Sciences, Vol. 24, No. 8, August, 1957.

39. Y. C. Fung and E. E. Sechler, "Buckling of Thin-Walled Circular Cylinders under Axial Compression and Internal Pressure," Journal of the Aeronautical Sciences, Vol. 24, No. 5, pp. 351-356, May, 1957.

40. W. S. Goree, "Stability of Thin Shells Stabilized by a Soft Elastic Core," University of Florida, Thesis, August, 1960.

41. R. F. S. Hearmon, An Introduction to Applied Anisotropic Elasticity, Oxford University Press, 1961.

42. S. G. Lekhnitsky, Theory of Elasticity of an Anisotropic Elastic Body, Holden-Day, 1963.

43. S. A. Ambartsumyan, "Theory of Anisotropic Shells" NASA TTF-118, May, 1964.

44. S. Cheng and B. P. C. Ho, "Stability of Heterogeneous Aeolotropic Cylindrical Shells under Combined Loading," Journal of the American Institute of Aeronautics and Astronautics, Vol. 1, No. 4, pp. 892-898, April, 1963.

BIOGRAPHICAL SKETCH

The author was born on December 5, 1934, in Fukien, China. He graduated from Taipei Middle School and then received his B.Sc. degree in Civil Engineering in 1957 at Taiwan Provincial Cheng Kung University, Tainan, Taiwan, China. During the period from August, 1957, to February, 1959, he served in the Army of the Republic of China, and then worked for the Civil Engineering Department of the Taiwan Provincial Taipei Institute of Technology as a teaching assistant from February, 1959, to August, 1960. In September, 1960, he was enrolled in the Graduate School of the University of Florida and received the degree of Master of Science with a major in Engineering Mechanics in June, 1962.

Since September, 1962, he has pursued his work toward the degree of Doctor of Philosophy in the Department of Engineering Science and Mechanics. During this period, he has been engaged in research activities in the Department of Engineering Science and Mechanics.

He is married to the former Lydia Rong-jang Hsu at Gainesville, Florida.

This dissertation was prepared under the direction of the chairman of the candidate's supervisory committee and has been approved by all members of that committee. It was submitted to the Dean of the College of Engineering and to the Graduate Council, and was approved as partial fulfillment of the requirements for the degree of Doctor of Philosophy.

August, 1965

R Martin
Dean, College of Engineering

Dean, Graduate School

Supervisory Committee:

S. J. Lu
Chairman

Herbert E. Hoagland

T. Lickman

W. A. Nash

R. G. McCabe